Next-generation automotive materials: Performance-driven yucca fiber reinforced PA11 bio-composites

Mohamed Amine Kacem, Laura Aliotta, Vito Gigante, Nassila Sabba, Sylvie Masse, Mahdi Bodaghi

International Journal of Biological Macromolecules 341 (2026) 150306

Contents lists available at ScienceDirect

International Journal of Biological Macromolecules

journal homepage: www.elsevier.com/locate/ijbiomac

Next-generation automotive materials: Performance-driven yucca fiber reinforced PA11 bio-composites

Mohamed Amine Kacem [a], Laura Aliotta [b,*], Vito Gigante [b], Nassila Sabba [c], Sylvie Masse [d], Mahdi Bodaghi [a,*]

[a] Department of Engineering, School of Science and Technology, Nottingham Trent University, NG11 8NS, Nottingham, UK
[b] Department of Civil and Industrial Engineering, University of Pisa, 56122, Pisa, Italy
[c] Laboratory of Matter's Valorization and Recycling for Sustainable Development, USTHB, 16111, Alger, Algeria
[d] Sorbonne Université, CNRS, Laboratoire de Chimie de la Matière Condensée de Paris, F-75005, Paris, France

ARTICLE INFO

Keywords:
Polyamide 11
Bio-composites
Yucca fibers
LCA
Humidity impact
Injection molding

ABSTRACT

Developing sustainable engineering materials requires systems that merge renewable origin, mechanical resilience, thermal stability, and industrial scalability. In this study, bio-based polyamide 11 (PA11) was reinforced with yucca fibers extracted via two eco-designed routes, traditional (YT) and water retting (YWR), to create next-generation bio-composites processed through injection molding. The incorporation of yucca fibers significantly enhanced the mechanical properties of PA11. Traditionally extracted fiber-reinforced composite (PA11-YT5) enhanced tensile (35.02 MPa) and flexural strengths (43.08 MPa) compared to 34.83 MPa and 41.81 MPa for neat PA11. Meanwhile, the water-retted composites (PA11-YWR5) exhibited accepted strength (34.75 MPa in tensile, and 41.84 MPa in flexural) with greater impact resistance and improved thermal stability. Enhancing the Heat Deflection Temperature (HDT) is key for enabling bio-composites to operate in thermally demanding applications. Here, yucca reinforcement markedly improved thermal resistance: the neat matrix showed an HDT of 72.25 °C, while fiber incorporation increased it by +52% (PA11-YT5%) and + 55% (PA11-YWR5%). After hygrothermal aging (37 °C, 85% RH, 30 days), both systems retained over 98% of their initial strength in tensile, demonstrating high environmental durability. Life cycle assessment (i.e., LCA) confirmed a lower carbon footprint (≈1.27 kg CO_2 eq./kg) and reduced processing energy relative to neat PA11. The results of this study highlight yucca fibers as a compelling renewable alternative to widely used natural fibers, providing consistent mechanical reinforcement and notable thermal stability. Combined with their environmental advantages, these characteristics position yucca fibers as attractive candidates for sustainable automotive components and lightweight structural applications.

1. Introduction

In the context of global imperatives to mitigate the environmental impact of materials and reduce dependence on finite fossil-based resources, the development of sustainable polymer systems has become a central focus of scientific research and industrial innovation. Bio-based materials, which integrate polymers derived from renewable plant sources with lignocellulosic reinforcements, serve as a cornerstone of eco-design paradigms [1]. These paradigms aim to engineer high-performance, lightweight materials that adhere to the principles of a circular economy, thereby minimizing environmental impacts across the entire life cycle, from raw material extraction and processing to end-of-life management, including recycling or biodegradation [2].

In the realm of advanced materials science, bio-composites have emerged as a paradigm-shifting class of materials, offering sustainable alternatives to conventional composites reinforced with synthetic polymers and mineral fibers [3]. Distinguished by their low density, adjustable biodegradability based on compositional tailoring, and significantly reduced carbon footprint, bio-composites offer substantial promise for the development of high-performance technical components, particularly in automotive applications [4]. Within this industry, the reduction of structural mass is paramount, directly contributing to improved energy efficiency and decreased greenhouse gas emissions [5]. The robust mechanical properties of bio-composites, coupled with

* Corresponding authors.
E-mail addresses: laura.aliotta@unipi.it (L. Aliotta), mahdi.bodaghi@ntu.ac.uk (M. Bodaghi).

https://doi.org/10.1016/j.ijbiomac.2026.150306
Received 7 December 2025; Received in revised form 11 January 2026; Accepted 13 January 2026
Available online 14 January 2026

their compatibility with advanced fabrication techniques, such as injection molding and compression molding, enable them to meet the stringent performance and environmental criteria required for structural applications. These attributes align seamlessly with international regulatory frameworks and global carbon neutrality goals, positioning bio-composites as a transformative material class for sustainable engineering solutions [6,7].

In this context, polyamide 11 (PA11), a bio-derived semicrystalline thermoplastic synthesized from renewable castor oil, is renowned for its superior thermal stability, chemical inertness, high impact toughness, and recyclability, distinguishing it from conventional fossil-based polyamides [8]. These attributes, coupled with its reduced environmental footprint, position PA11 as an exemplary material for sustainable engineering applications. To extend its utility in high-performance components subjected to complex mechanical loading, the integration of reinforcing fibers is imperative to enhance its mechanical properties, such as tensile strength and modulus [9]. These properties render PA11-based bio-composites a high-performance, eco-friendly solution for automotive and construction sectors, supporting global sustainability and carbon neutrality objectives [10].

Natural fibers, as fundamental components of bio-composites, critically govern the material's overall performance. Their mechanical, physical, and chemical properties are profoundly influenced by the extraction methodology employed [11]. Techniques such as mechanical decortication, chemical retting, or biological enzymatic processing profoundly influence fiber properties, including morphology, cellulose fraction, degree of crystallinity, and surface chemical composition. These factors directly modulate the efficacy of fiber-matrix interfacial bonding, a determinant of composite mechanical integrity. Rigorous studies emphasize that tailored modulation of extraction parameters is paramount for enhancing fiber characteristics and hence composite performance. Consequently, this variability underscores the imperative for advanced research in natural fiber engineering to systematically optimize their structural, chemical, and interfacial properties, thereby enabling bespoke solutions for high-performance applications in bio-composite materials [12,13].

The investigation of lignocellulosic fibers for bio-composite applications has identified yucca fiber, derived from *Yucca aloifolia* L., as a promising reinforcement due to its high cellulose content, robust microstructural architecture, and prevalence in arid regions known for its drought tolerance and robust growth in sandy, well-drained soils [11]. This species, commonly referred to as Spanish bayonet, features long, rigid, sword-shaped leaves typically measuring 60–120 cm in length, 3–6 cm in width, and 0.5–1 cm in thickness, with a fibrous internal structure rich in cellulose. These leaves yield fibers with high tensile strength and a favorable lignocellulosic composition, yet their integration in PA11-based bio-composites remains underexplored. In contrast to flax, hemp, sisal, and kenaf fibers that have attracted sustained scientific attention due to their long-standing agricultural cultivation, wide commercial availability, and well-documented mechanical and chemical properties, yucca fibers remain largely unexplored in materials research. The limited attention is due to their historical use in artisanal applications and their natural prevalence in arid and semi-arid ecosystems, where limited industrial cultivation has constrained systematic materials research. Consequently, systematic studies of yucca in high-performance polymer matrices such as PA11 are scarce, representing a critical knowledge gap that this work aims to address. The selection of PA11 as the polymer matrix is deliberate, unlike to polylactic acid (PLA), which suffers from rapid hydrolytic degradation, or polypropylene (PP), which lacks the necessary thermal and structural resilience, PA11 combines long-term mechanical stability, chemical resistance, and high processability, making it uniquely suited for functional, load-bearing, and semi-structural applications. By integrating yucca into PA11, this work not only advances the development of high-performance, sustainable bio-composites but also demonstrates a design philosophy where renewable materials can meet the rigorous demands of automotive, aerospace, and advanced engineering applications. However, the efficacy of yucca fiber as a reinforcement phase is critically dependent on the extraction technique, which dictates fiber morphology, crystallinity, lignocellulosic composition, and surface chemistry, thereby influencing interfacial adhesion with the polymeric matrix [14]. Strategic refinement of extraction methods, such as selective traditional or enzymatic processing, is imperative to optimize fiber-matrix interactions and enhance the mechanical performance of the resulting composites. Although yucca fibers exhibit attractive intrinsic properties for sustainable reinforcement, current studies largely overlook the role of fiber extraction pathways in governing the processing-structure-property relationships of PA11-based bio-composites. In particular, the absence of systematic comparisons between traditional extraction and controlled water retting under industrially relevant processing conditions, such as injection molding, hinders a predictive understanding of fiber-matrix interactions and composite performance. Addressing this gap is critical for translating yucca fiber-reinforced PA11 systems from laboratory-scale demonstrations to scalable engineering applications.

Extensive research on natural fiber-reinforced bio-composites revealed a broad spectrum of mechanical properties, governed by fiber type, polymer matrix, and elaboration techniques. As noted, composites utilizing flax and hemp fibers in PLA or PP matrices demonstrate tensile strengths of 30–80 MPa, Young's moduli ranging from 3 to 9 GPa, and fracture toughness significantly modulated by fiber-matrix interfacial adhesion [15,16]. Similarly, jute fiber reinforced PP composites demonstrate comparable tensile strengths of 35 MPa, with elastic moduli of 3.4 GPa, influenced by fiber content [17]. Additionally, yucca fiber composites in PLA matrices have been reported to achieve tensile strengths of 40–60 MPa and moduli around 1.3 GPa, with performance contingent on fiber volume fraction and extraction method conditions [18]. These properties, typically expressed as ranges from 30 to 80 MPa, underscore the potential of natural fibers to rival synthetic reinforcements, provided processing parameters are precisely optimized to enhance interfacial bonding and overall composite performance.

These bio-composites typology can find suitable applications in the automotive industry since it is at the forefront of adopting more sustainable materials to meet stringent environmental regulations and performance demands. The integration of bio-composites into interior and semi-structural components to enhance sustainability and reduce vehicle mass represent a valuable approach for increasing vehicles' sustainability [19]. For instance, BMW incorporated kenaf fiber-reinforced composites in door panel assemblies, while Mercedes-Benz utilized flax-based composites for dashboard frameworks and hemp-kenaf blends for sunroof frames, achieving up to 50% weight reduction compared to metal counterparts [20]. In addition, Toyota employed polypropylene (PP)/kenaf composites in door trims of sustainable concept vehicles, and Ford integrated kenaf-reinforced polypropylene in interior panels of models like the Mondeo, alongside castor oil-based plastics for fuel lines [4]. Volvo leveraged flax-based composites from Bcomp's ampliTex for dashboard and door trims in the EX30, reducing plastic content by up to 70%, and Audi incorporated sisal-reinforced composites in floor mats and flax-based materials in the A2's parcel shelves [21]. Finally, also Stellantis applied hemp-polypropylene composites in Jeep Cherokee door panels, leveraging their low density and recyclability. These applications underscore the industry's focus on reducing vehicle mass to enhance fuel efficiency also complying with the carbon neutrality sustainability goals [22]. Transitioning from natural sources to industrial applications, the incorporation of these materials into functional components represents a pivotal step toward their validation and large-scale implementation, as illustrated in Fig. 1.

In this context, this study advances the development of high-performance bio-composites comprising PA11 reinforced with yucca fiber powder, extracted through traditional mechanical processing and water retting, and fabricated via micro compound injection molding at fiber loadings of 3 wt% and 5 wt%. The study pursues dual objectives,

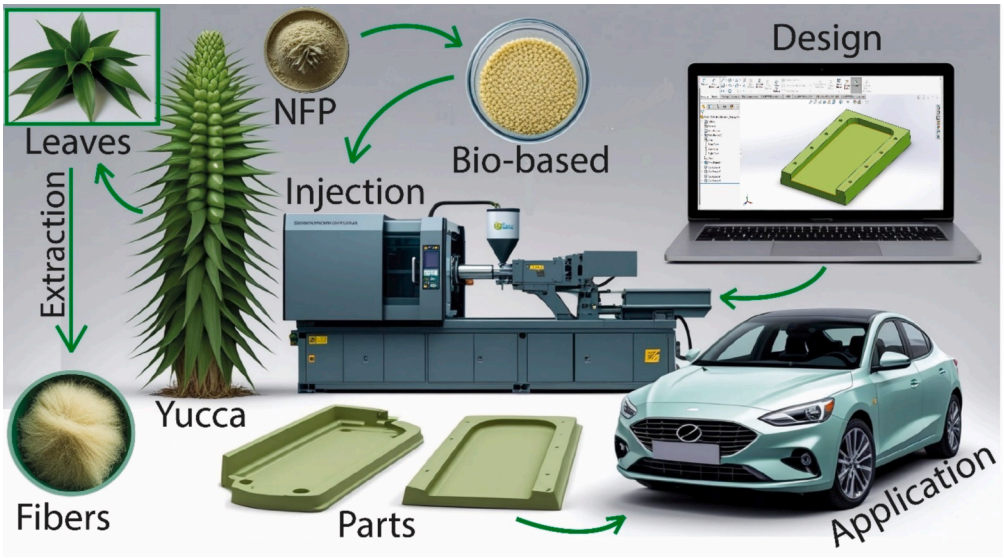

Fig. 1. - Overview of the manufacturing stages of injection-molded bio-composites for automotive components. (NFP is Natural Fibers Powder).

the primary objective is to systematically elucidate the effects of extraction techniques and fiber concentrations on the composites' microstructural integrity, thermal stability, and mechanical performance, employing scanning electron microscopy (SEM) for morphological analysis, differential scanning calorimetry (DSC) for thermal behavior, heat deflection temperature (HDT) testing load to assess thermal resistance, tensile, flexural, and impact testing for mechanical characterization, as well as dynamic mechanical analysis (DMA) for viscoelastic behavior assessment. Secondly, the composites' response to humid environments is evaluated to ensure compliance with automotive durability standards. Furthermore, this work significantly contributes to the development of PA11-yucca fiber bio-composites for next-generation automotive applications, aligning with global decarbonization and sustainability imperatives.

2. Materials and methods

2.1. Fibers extraction methods from yucca plant and leaves

Yucca plants (*Yucca aloifolia* L., Asparagaceae) sourced from semi-arid regions of Algeria, more exactly in Hadjout city with exact geographic coordinates at 36° 30′ 44.787″ N 2° 24′50.859″ E, leveraging their natural abundance and robust lignocellulosic structure. Mature leaves, selected for uniform dimensions, structural integrity, and absence of damage or disease, were segmented into around 30 cm lengths to optimize handling during extraction. These segments were meticulously washed with deionized water to remove surface contaminants, including dust, soil, and microbial residues, and air-dried at 25 °C to preserve fiber quality. This preparation ensured consistent feedstock for subsequent mechanical processing and water retting, enabling reliable extraction of yucca fiber powder for bio-composite fabrication.

Natural yucca fibers were extracted from *Yucca aloifolia* L. leaves using two distinct methods, traditional mechanical processing and water retting biological technique. For mechanical extraction, fresh leaves underwent hydrothermal pretreatment in water at 80 ± 1 °C for 1 h to destabilize lignocellulosic interfaces, enabling efficient fiber liberation. A calibrated scraping apparatus was then utilized to selectively remove non-fibrous constituents, yielding high-purity fiber fascicles. These were subjected to sequential washing with deionized water to eliminate residual organic detritus and inorganic particulates, followed by controlled air-drying at 25 ± 1 °C in a low-humidity chamber (<40% RH to safeguard cellulose microfibril integrity). Conversely, water retting involved submersion of leaves in river-water for 35 ± 1 days at 20–25 °C, harnessing microbial enzymatic hydrolysis to cleave pectin linkages and isolate fibers. Post-retting, fibers were rigorously washed, solar-dried under ambient conditions, and stored less than 8% RH to prevent degradation. Moreover, although the 35-day water retting period is effective at laboratory scale, it could be shortened at industrial scale by employing targeted enzymatic cocktails or engineered microbial strains. These microorganisms selectively attack non-cellulosic components, such as pectin and hemicellulose, accelerating fiber liberation while preserving the cellulose-rich structure. Such strategies could significantly reduce retting duration, improving scalability and reproducibility for natural fibers production.

Both fiber cohorts were micronized using a high-energy knife mill, followed by sieving through a 100-mesh stainless steel screen (aperture 150 ± 3 μm) to achieve a tightly controlled fibers particle size distribution (≤150 μm). The resultant fiber powder was dehydrated in a convection oven at 60 ± 2 °C for 24 h, to eliminate residual moisture, ensuring suitability for incorporation into polyamide 11 (PA11) bio-composites via injection molding.

2.2. Bio-composite preparation

Bio-based polyamide 11, was purchased by NaturalPlast (Ifs, France), with the trade name NP BioPA11–254 [MVR (235 °C, 2.16 kg) = 30 cm^3/10 min, density = 1.03 g/cm^3). This grade was chosen because it is specifically designed for injection molding applications. This PA11 grade served as polymer matrix for the fabrication of the bio-composites, integrated with yucca fiber powder at 3 wt% and 5 wt% fractions extracted via water-retting (PA11-YWR) and traditional methods (PA11-YT), to exploit its lignocellulosic chemistry. Before melt processing bio-PA11 pellets were dried in a ventilated oven at 80 ± 0.5 °C for 24 h. Melt compounding was carried out in a Thermo Scientific HAAKE MiniLab II micro-compounder (Thermo Fisher Scientific Inc., Waltham, USA) with co-rotating conical twin screws, maintained at 210 °C and 130 rpm. A 120 s closed-loop recirculation cycle facilitated molecular-level dispersion of yucca fibers, monitored via real-time torque (Nm) and melt pressure (bar) to validate uniform chemical integration and viscosity stability. Upon completion of the blending cycle, the molten material was transferred, through a preheated cylinder (set at the same extruder temperature of 210 °C), to a Thermo Scientific Haake MiniJet II mini- injection moulder. For clarity, a complete nomenclature of the tested bio-composites, including fiber extraction method, and concentrations is provided in Table 1 to facilitate interpretation of the results.

Table 1
Sample identification and experimental matrix for PA11/Yucca fiber bio-composites.

Matrix	Natural fiber	Extraction method	Fiber content [%]	Designation
PA11	–	–	–	Pure PA11
PA11	Yucca	Water retting	3	PA11-YWR3
PA11	Yucca	Water retting	5	PA11-YWR5
PA11	Yucca	Traditional	3	PA11-YT3
PA11	Yucca	Traditional	5	PA11-YT5

The molding process within the Haake MiniJet II mini- injection moulder was conducted at 210 °C under and molding temperature of 60 °C. Injection parameters were expertly calibrated to accommodate the two distinct mold geometries adopted. Tensile specimens (Haake type III dog-bone tensile specimens 25 × 5 × 1.5 mm) were molded at 500 bars, whereas flexural, HDT, and Charpy impact (ISO 179 Type D parallelepiped specimens 10 × 80 × 4 mm) specimens required 670 bar to achieve uniform packing due to the higher number of materials used for this specimen typology. An injection duration of 7.0 s was uniformly applied to minimize variability and ensure morphological homogeneity. Post-molding, specimens were in-mold cooled to ambient temperature, demolded, and stored in a controlled desiccated environment (25 °C, <10% RH) to prevent moisture-driven chemical modifications, preserving their integrity for subsequent physicochemical and mechanical analyses. In addition, Fig. 2 provides a concise overview of the injection molding pathway engineered for precise fabrication of PA11 and PA11/Yucca composite specimens.

2.3. Bio-composite characterization

2.3.1. Morphology evaluation

The morphology and fiber-matrix interface of the PA11-yucca bio-composites were examined using an EM-30 Scanning Electron Microscope (Coxem Ltd., Daejeon, Korea). Fractured tensile specimens were cryo-fractured in liquid nitrogen to preserve microstructural features and subsequently gold-coated using an Edward S150B sputter coater (BOC Edwards, UK) to avoid charge build up. This microstructural investigation aimed to evaluate the yucca fibers dispersion and the interfacial bonding quality within the PA11 matrix, with particular attention to the influence of different fiber extraction methods. The SEM observations enabled the identification of key morphological markers, including fiber pull-out, interfacial debonding, void formation, and evidence of resin infiltration into the fiber structure.

2.3.2. Mechanical performance evaluation

The mechanical performance of the pure PA11 and PA11-yucca bio-composites were evaluated through tensile, flexural, and impact tests, in accordance with the relevant ISO standards. Tensile test was conducted following ISO 527-2 using a universal testing machine (Zwick 8306, equipped with a 2.5 kN load cell) at a crosshead speed of 2 mm/min. Flexural properties were assessed according to ISO 178 (three-point bending mode) at the same crosshead speed (2 mm/min), using a universal testing machine (ZwickiLine, equipped with a 2.5 kN load cell). Charpy impact tests were conducted in notched configuration, according to ISO 179, on Instron CEAST 9050 machine (INSTRON, Canton, MA, USA) equipped with a 15 J Charpy pendulum (45°notch, 2 mm depth, and 0.25 mm radius of curvature at the base of the notch). All mechanical tests were performed under controlled laboratory conditions at 23 ± 2 °C and 50 ± 5% relative humidity.

For each mechanical test, five replicates per formulation were carried out and the average values and standard deviations of the measured parameters reported.

2.3.3. Heat deflection temperature (HDT) assessment

Evaluating the thermal endurance of bio-based composites under mechanical load is crucial for assessing their suitability in high-performance applications. The Heat Deflection Temperature (HDT) test was therefore conducted to quantify the thermomechanical stability of PA11-yucca bio-composites. Rectangular specimens with dimensions of 80 mm × 10 mm × 4 mm were used for this test. The experiments were conducted using an HDT apparatus (HVT302B, MP, Milan, Italy) in a three-point bending configuration. Each specimen was positioned flatwise in a silicone oil bath and subjected to a constant flexural stress of 0.45 MPa at the midpoint. The bath temperature was increased at a controlled rate of 120 °C h^{-1} in accordance with ISO 75, Type B standard. The test was terminated once the central deflection reached 0.34 mm, corresponding to the standard deformation criterion. Three specimens were tested for each material composition, and the average HDT value reported.

2.3.4. Thermal properties assessment

The materials thermal properties (e.g. thermal transitions and crystallinity behavior) of the PA11-yucca bio-composites were characterized using TA-Q200 DSC (TA Instruments, New Castle, DE) using nitrogen as purge gas set at 50 mL/min. The sampling was carried out by cutting about 10–15 mg of material from molded dog-bone samples; each sample was then sealed in aluminum pans and subjected to the thermal program. To consider the effect of the injection molding process, only one heating run at 10 °C/min from room temperature up to 210 °C. From the obtained thermograms, the glass transition temperature (T_g), melting temperature (T_m), and melting enthalpy (ΔH_m) were recorded. The degree of crystallinity (X_c) of the PA11 matrix in the composites was

Fig. 2. Fabrication route of injection-molded PA11/Yucca composite specimens.

calculated using the following equation (Eq. 1):

$$X_c(\%) = \frac{\Delta H_m}{\Delta H_m^0 \times W_{PA11}} \times 100 \quad (1)$$

In this context, ΔH_m is the measured melting enthalpy (J/g), ΔH_m^0 is the melting enthalpy of 100% crystalline PA11 (taken as 226.4 J/g [23]), and W_{PA11} is the weight fraction of PA11 in the composite.

2.3.5. Dynamic mechanical analysis

The dynamic mechanical properties of neat PA11 and PA11 composites reinforced with yucca fibers were evaluated by dynamic mechanical thermal analysis (DMTA), in tensile configuration. DMTA tests were performed using a Gabo Eplexor® DMTA (NETZSCH Group, Bavaria, Germany) equipped with a 100 N load cell. Each formulation was tested with at least three specimens. Test bars (20 × 5 × 1.5 mm) were obtained by cutting rectangular sections from tensile specimens. The tests were carried out at a constant frequency of 1 Hz sweeping the temperature from −50 up to 120 °C with a heating rate of 1.5 °C/min. This analysis aimed to investigate the viscoelastic behavior of the materials and to understand the reinforcing effect of yucca fibers on the molecular mobility and relaxation processes of the PA11 matrix. The storage modulus (E′), correlated to the elastic properties of the material, and the damping factor (tan δ), correlated to the polymeric chain mobility and glass transition temperature, were recorded.

2.4. Humidity effects on performance of bio-composites

To investigate the durability and the performance of pure PA11 composite and PA11-yucca bio-composites under environmental stress, a robust hygrothermal conditioning protocol was executed in strict accordance with ASTM D5229/D5229M. Triplicate specimens for each formulation were subjected to a precisely controlled climate chamber at 38 ± 0.5 °C and 85 ± 1% relative humidity (RH) for a duration of 30 days. These conditions were judiciously optimized to replicate the environmental stresses of automotive interior applications, accelerating moisture diffusion while ensuring fidelity to real-world service scenarios. This rigorous protocol enabled precise quantification of water absorption kinetics and their profound effects on the bio-composites' mechanical performances.

2.4.1. Water absorption kinetics

During the hygrothermal conditioning in a climate chamber set at 38 ± 0.5 °C and 85 ± 1% relative humidity (RH) for 30 days, the water absorption behavior of pure PA11 and PA11-yucca bio-composites were evaluated following ASTM D570–98. The samples of each category were initially weighed to determine the dry mass (W_0) using a precision balance (±0.001 mg accuracy). Throughout the 15-day conditioning period, each specimen was removed periodically every 24 h, surface-dried with a lint-free cloth, and reweighed to record the wet mass (W_t). The water absorption percentage, M_t, was calculated as:

$$M_t(\%) = \frac{W_t - W_0}{W_0} \times 100 \quad (2)$$

Where W_t is the mass at time t, and W_0 is the initial dry mass.

To describe the moisture diffusion kinetics, the experimental data were fitted using Fick's second law of diffusion for thin plates, assuming one-dimensional transport and negligible swelling effects [24]. For short-time diffusion (Mt/M∞ < 0.5), the relationship between relative uptake and time follows:

$$\frac{M_t}{M_\infty} = 4\left(\frac{Dt}{\pi h^2}\right)^{1/2} \quad (3)$$

where D_{app} is the apparent diffusion coefficient ($m^2 \cdot s^{-1}$) and h is the specimen thickness. The diffusion coefficient was determined from the slope (k) of the linear region of the curve $Mt/M\infty$ versus $\sqrt{t}$, according to:

$$D_{app} = \frac{\pi}{16}\left(\frac{kh}{M_\infty}\right)^2 \quad (4)$$

This approach enables quantitative comparison of water transport mechanisms among the neat and reinforced systems, linking the diffusion behavior to the fiber-matrix interfacial architecture and microstructural features.

2.4.2. Post-conditioning mechanical response

Upon completion of the 30-day hygrothermal conditioning, the mechanical performance of pure PA11 and PA11-yucca bio-composites was rigorously evaluated to quantify the effects of moisture exposure. Triplicate specimens (3), prepared in accordance with the relevant ISO standards for each formulation, were tested after conditioning and compared with unconditioned control specimens. Tensile and flexural tests were conducted under the same parameters and using the same equipment as described for the dry-state analysis (Section 2.3.2). The results provide clear insight into the influence of hygrothermal aging on mechanical properties, thereby enhancing the understanding of bio-composite stability for sustainable applications.

2.5. Bio-composite cradle-to-gate LCA and real application

In order to complement the experimental characterization, a preliminary cradle-to-gate life cycle assessment (LCA) and cost evaluation were conducted to quantify the environmental and economic feasibility of the developed PA11-yucca bio-composites in accordance with ISO 14040 and ISO 14044 guidelines. This methodological step was undertaken to link the technical performance of the PA11-yucca bio-composites with their potential environmental and economic impacts, providing a decision-support basis for future industrial adoption.

For fibers obtained via traditional extraction, the thermal energy demand was estimated using the following eq. (5):

$$Q = \frac{m \times C_p \times \Delta T}{\eta} \quad (5)$$

In this context, m is the mass of water, C_p is the specific heat capacity of water (4.18 kJ/kg·°C), ΔT is the temperature rise, and η is heating system efficiency (η = 0.8, assuming 80% heating system efficiency), providing the actual energy consumption used in the LCA estimation.

The cradle-to-gate carbon footprint of the bio-composite was then calculated as:

$$CF_{composite} = (W_{PA11} \times EF_{PA11}) + (W_{fiber} \times EF_{fiber}) + \sum_{i=1}^{n} (E_i \times EF_E) \quad (6)$$

Here, $CF_{composite}$ is total carbon footprint of the bio-composite (kg CO_2 eq./kg), W_{PA11} and W_{fiber} are the respective masses of PA11 matrix and yucca fibers in the composite, EF_{PA11} and EF_{fiber} their emission factors (kg CO_2 eq. /kg),and $(E_i \times EF_E)$ are emissions associated with processing steps (grinding) expressed in kg CO_2 eq.

In parallel, a preliminary cost analysis was carried out using equation number (7):

$$C_{total} = (W_{PA11} \times P_{PA11}) + (W_{fiber} \times P_{fiber}) + (E_{process} \times P_{electricity}) \quad (7)$$

In this equation, P_{PA11} and P_{fiber} are the market prices of PA11 and yucca fibers (€/kg). The unit price of PA11 was considered to be 9 €/kg, while the powdered yucca fibers were priced at 4 €/kg for the WR type and 3 €/kg for the T type. $E_{process}$ and $P_{electricity}$ represent the process energy demand (kWh) and local electricity cost (0.22 €/kWh), respectively.

All input parameters and emission factors used for these calculations were sourced from open databases and peer-reviewed literature [25,26],

ensuring transparency and reproducibility of the LCA and cost estimations.

3. Results and discussion

3.1. Microstructural observations and surface characterization

As an initial step in the characterization process, SEM observations were performed in order to gain a fundamental understanding of the microstructural architecture of the PA11-yucca bio-composites. This early examination focused on the distribution of the yucca fibers within the matrix and the quality of the fiber-matrix interface, allowing the identification of relevant fracture features such as fiber pull-out, interfacial debonding, voids, and evidence of resin infiltration. Representative micrographs for both PA11 bio-composites rienforced via water-retted (PA11-YWR) and traditionally extracted (PA11-YT) are presented in Fig. 3, providing direct visual evidence of the influence of extraction method on the integrity of the fiber-matrix interface. Yucca fiber morphology in both category are illustrated in Fig. 4. The morphological information obtained at this stage served as a basis for interpreting the trends observed in the subsequent mechanical and thermal performance, providing a clear link between processing conditions, internal structure, and overall composite behavior.

The bio-composites SEM micrographs (Fig. 3) offer critical insights into the microstructural mechanisms that govern the load transfer and durability of the PA11-yucca bio-composites. In the PA11-YWR series, the fibers are generally well embedded within the PA11 matrix, yet small interfacial gaps can be observed surrounding yucca fibers (Fig. 3A). This characteristic is linked to the water-retting extraction method, which produces fibers with smoother surfaces and fewer surface irregularities [27], as illustrated in Fig. 4A. Such smooth surfaces inherently offer fewer anchoring points and less mechanical interlocking potential. In addition, the limited surface roughness may reduce the number of accessible functional groups, thereby limiting physical interactions with the matrix and leaving micro-scale cavities at the interface [28]. These micro-gaps, even though minimal, can act as sites for localized stress concentration under service conditions or pathways for moisture ingress during long-term aging [29]. In contrast, the PA11-YT series reveals a markedly different morphology. The fibers extracted by the traditional method show a highly textured surface with visible micro-porosities (Fig. 4B). This rougher surface provides a significantly larger effective contact area, allowing the matrix to better penetrate and conform to the fiber surface [30]. The abundant surface asperities and pores enhance mechanical interlocking, while also offering more potential sites for secondary physical or chemical interactions [31,32]. As a result, SEM analysis of the PA11-YT bio-composite, as depicted in Fig. 3B, reveals fibers that are seamlessly and tightly integrated within the polymer matrix, exhibiting no discernible interfacial voids, gaps, or discontinuities. This intimate fiber-matrix integration underscores a robust interfacial bond, characterized by good adhesion properties. The absence of defects at the interface suggests a high degree of compatibility between the fiber and the matrix, likely resulting from optimized processing conditions or surface interactions that enhance molecular interlocking [33,34]. Such a strong interface is critical for ensuring resistance to fiber debonding or delamination, both during manufacturing processes and under in-service mechanical or environmental stresses [35].

Furthermore, across both extraction methods, the micrographs reveal well-integrated fibers within the PA11 matrix, primarily intended to examine fiber-matrix cohesion. During SEM analysis, the dispersion of fibers into PA11 was qualitatively inspected, although no dedicated images were captured for this purpose, the relatively low fiber contents (3 wt% and 5 wt%) likely prevented agglomeration and promoted uniform resin infiltration [36]. Such homogeneity at the microscale is a critical prerequisite for achieving consistent and reliable composite behavior. Although the current microstructure is already promising, the presence of micro-voids in the PA11-YWR interface suggests potential for further improvement. Surface modification strategies, such as the application of a suitable coupling agent as well as chemical treatments, could be employed to introduce additional reactive sites or enhance wettability, thereby minimizing interfacial gaps and further strengthening the fiber-matrix integration [37,38]. These targeted adjustments would support the development of even more stable and durable bio-composite interfaces, advancing their potential for demanding industrial applications.

3.2. Thermal behavior and molecular ordering

The thermal properties of polyamide 11 and its bio-composites reinforced with 3 wt% and 5 wt% yucca powder, extracted via traditional method (T) and water-retting method (WR), were characterized using Differential Scanning Calorimetry (DSC). The results, presented in Fig. 5 and summarized in Table 2, include the glass transition temperature (Tg), melting temperature (Tm), melting enthalpy (ΔH_m), and degree of crystallinity (Xc), providing insights into the influence of yucca powder and its extraction method on the thermal behavior of the PA11 matrix.

Differential scanning calorimetry reveals that incorporating yucca-derived powders into the PA11 matrix induces subtle yet meaningful modifications in the polymer's thermal transitions and crystalline organization. Pure PA11 exhibits a glass transition at 47.8 °C and a melting temperature of 192.4 °C, consistent with literature values for semi-crystalline long-chain aliphatic polyamides [39]. Upon the introduction of yucca powders, regardless of extraction pathway (water retting or traditional), a systematic decrease in Tg is observed, falling to 44.6–45.3 °C across all composite formulations. This decrease indicates a slight enhancement of local chain mobility within the amorphous regions, likely due to the introduction of interfacial free volume between the polymer and the dispersed lignocellulosic particles [40]. Such behavior reflects the dual role of natural fibers, while acting as

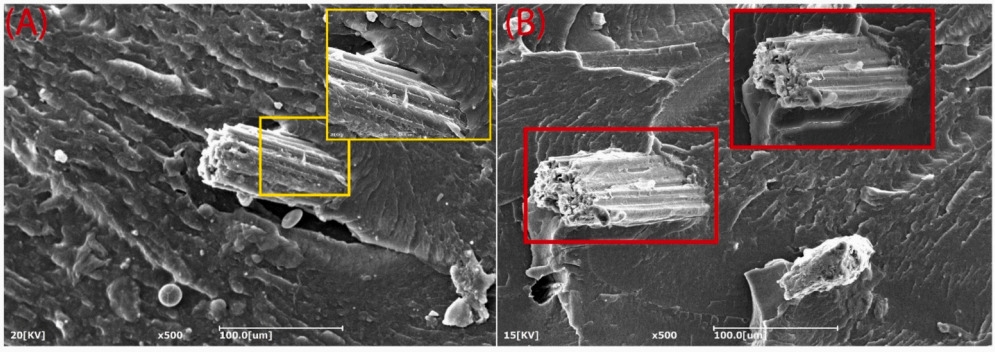

Fig. 3. Fiber-matrix interfaces under SEM. (A) and (B) PA11-YWR and PA11-YT bio-composites types.

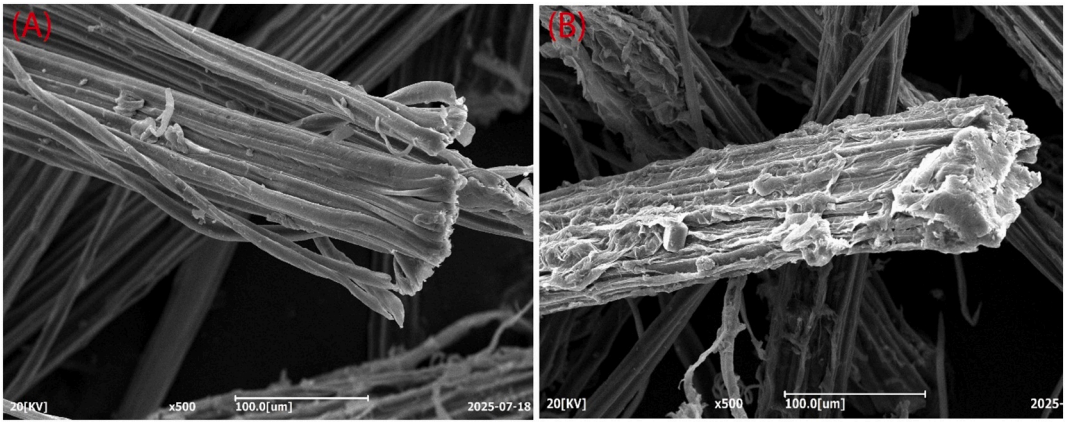

Fig. 4. Yucca natural fibers SEM micrographs. (A) and (B) Morphology of Yucca fiber extracted via water retting and traditional methods, respectively.

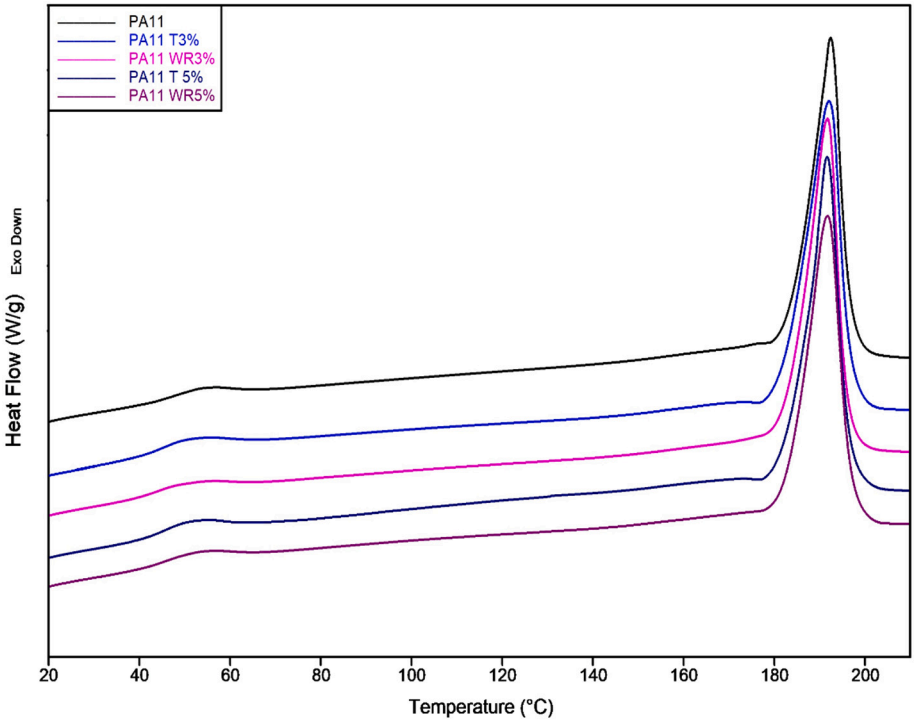

Fig. 5. Thermal Transition and crystallization behavior of PA11 and PA11/yucca bio-composites.

Table 2
Crystallinity and thermal behavior of PA11 and PA11-yucca systems.

Sample type	Glass transition temperature [°C]	Melting temperature [°C]	Melting enthalpy [J/g]	Degree of crystallinity [%]
Pure PA11	47.8	192.4	72.78	32.1
PA11-YWR3	44.6	191.7	74.04	33.7
PA11-YWR5	44.9	191.7	72.45	33.7
PA11-YT3	45.3	192.0	74.04	33.7
PA-11YT5	44.8	191.6	77.02	35.8

reinforcing agents, they can also locally perturb the polymer chain packing in amorphous domains [41].

Interestingly, the melting temperature (Tm) remains essentially unchanged (191.6–192.0 °C), demonstrating that the crystalline phase retains its α-PA11 lamellar structure without significant lattice perturbation [42]. However, variations in melting enthalpy (ΔH_m) and crystallinity reveal deeper structural implications. While Pure PA11 exhibits a melting enthalpy of 72.78 J/g corresponding to 32.1% crystallinity, the incorporation of yucca powders results in an overall enhancement of crystallinity, with values rising to 33.7% for most formulations and reaching a pronounced 35.8% for PA11-YT5. Consequently, the increase in crystallinity observed upon the incorporation of yucca-derived powders indicates that the fibers actively participate in the crystallization behavior of PA11 rather than acting as passive fillers. In this context, the fiber surfaces introduce interfacial constraints that locally restrict polymer chain mobility and, in turn, promote ordered chain alignment during cooling, thereby facilitating heterogeneous nucleation [43]. Importantly, this confinement-driven mechanism enhances crystallization while preserving the intrinsic crystalline structure of PA11, as confirmed by the stability of the melting temperature. Moreover, the

differences in crystallinity observed between extraction routes further underscore the pivotal role of fiber surface chemistry and morphology in governing polymer-fiber interactions. In particular, traditionally extracted fibers, which retain a higher density of exposed hydroxyl-rich polysaccharide domains, act as more efficient nucleation sites, leading to enhanced crystal growth and increased melting enthalpy. Notably, this effect becomes more pronounced at higher filler loadings, where the enlarged interfacial area amplifies nucleation efficiency [44]. As a direct consequence, these crystallization-driven microstructural evolutions translate into improved mechanical performance, wherein higher crystalline fractions contribute to enhanced stiffness and dimensional stability, while the well-developed interfacial regions promote more effective stress transfer under mechanical loading. The polysaccharide-rich micro-particulates act as heterogenous nucleation sites, lowering the thermodynamic barrier for crystal formation during melt cooling [45]. The effect is especially pronounced in PA11-YT5, where the highest concentration of extractive-rich, partially fibrillated particles appears to accelerate spherulitic development, leading to a more tightly packed crystalline framework. Moving forward, the melting enthalpy trend, peaking at 77.02 J/g in PA11-YT5, corroborates this nucleating behavior and suggests improved lamellar thickening or enhanced crystal perfection [46]. Such changes have profound implications for the mechanical performance: increased crystallinity often correlates with higher stiffness and thermal resistance, although it may also influence ductility depending on interphase adhesion and plasticization effects from amorphous restructuring.

From a materials-design perspective, these findings highlight the capacity of yucca-derived micro-powders to serve not only as fillers but also as functional crystallization modifiers in long-chain renewable polyamides. The synergistic interaction between lignocellulosic nucleates and bio-based PA11 aligns perfectly with ongoing efforts to engineer high-performance, fully bio-derived composite systems suitable for automotive and advanced engineering applications.

3.3. Reaction-to-stress of yucca-reinforced PA11

3.3.1. Stretching limits and Fiber efficiency

The mechanical response of the developed bio-composites was assessed per ISO 527-2 under uniaxial tension in order to evaluate the influence of dual-extracted yucca fibers on the stiffness, strength, and ductility of the PA11 matrix. Tensile strength, Young's modulus, and elongation at break were measured for five sample in each category. Results are presented in Fig. 6 and summarized in Table 3, providing a quantitative basis for evaluating the influence of fiber loading and extraction methods on composite behavior. In addition, Table 4 compares the performance of the PA11-yucca composites with other natural fiber-reinforced PA11 systems reported in the literature, providing a comprehensive overview of their mechanical behavior.

Table 3
Impact of dual yucca fiber extraction on the tensile strength and stiffness of sustainable PA11 bio-composites.

Samples category	Tensile strength [MPa]		Young's modulus [GPa]		Elongation [%]	
	Average	[SD]	Average	[SD]	Average	[SD]
Pure PA11	34.83	± 1.21	0.98	± 0.019	38.13	± 3.00
PA11-YWR3	33.63	± 0.85	1.13	± 0.015	35.90	± 5.05
PA11-YWR5	34.75	± 1.17	1.27	± 0.078	30.17	± 8.90
PA11-YT3	34.64	± 0.27	1.15	± 0.048	30.83	± 0.40
PA11-YT5	35.02	± 0.29	1.24	± 0.058	34.89	± 10.12

The tensile properties of PA11-yucca fiber bio-composites, as detailed in Table 3, reveal the nuanced interplay between fiber loading and extraction methodologies in modulating the mechanical response of the bio-based PA11 matrix, offering a robust dataset for advancing sustainable composite design. Pure PA11 exhibited a baseline tensile strength of 34.83 ± 1.21 MPa, Young's modulus of 0.98 ± 0.019, and elongation at break of 38.13 ± 3.00%, establishing a reference for unreinforced polymer behavior. Incorporation of 3 wt% water-retted yucca fiber in PA11 (PA11-YWR3) led to a tensile strength of 33.63 ± 0.85 MPa, a modest 3.45% decrease, which may be attributed to minor stress concentrations at the fiber-matrix interface caused by surface irregularities or residual non-cellulosic material from the retting process [47].

Table 4
Comparative mechanical performance of PA11 bio-composites reinforced with different natural fibers at varying concentrations.

Matrix	Natural filler	Concentration [%]	Tensile strength [MPa]	Young's modulus [GPa]	Reference
PA11	Yucca	5	35.02	1.24	This work
PA11	Wood	0.5	42	0.69	[58]
PA11	Spinifex	0.5	44	0.65	[58]
PA11	Cellulose Nanofibers	3	38	1.05	[59]
PA11	Jute	20	23.79	1.53	[60]

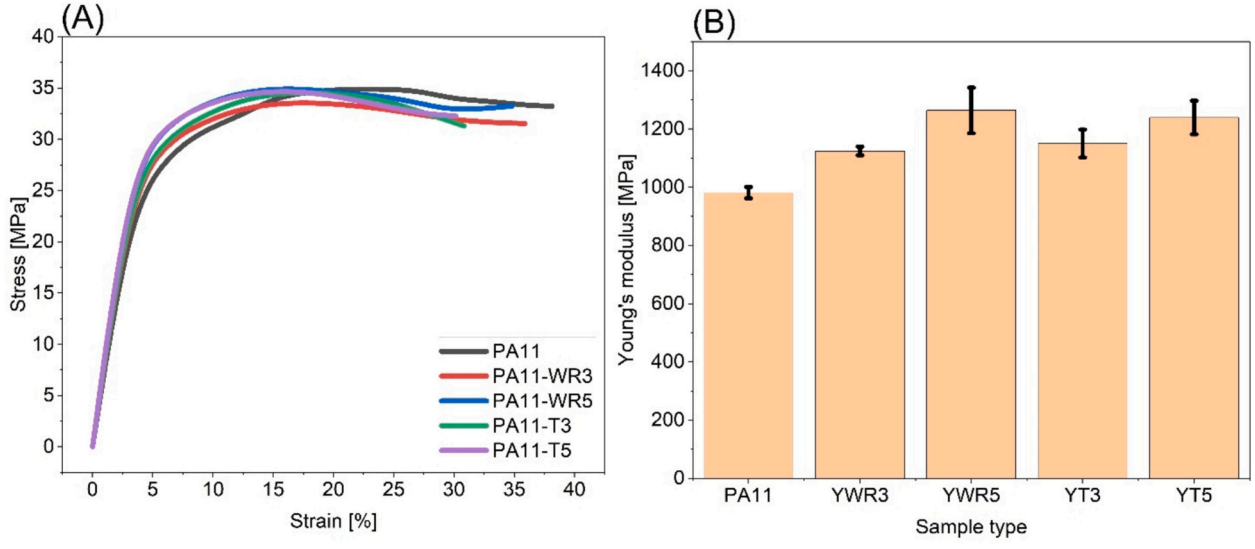

Fig. 6. Tensile response of PA11 bio-composites in dry state. (A) Stress-Strain curve, (B) Young's modulus histogram.

Nevertheless, Young's modulus increased by 14.58% to 1.13 ± 0.015 GPa, demonstrating a clear stiffening effect arising from the higher modulus of the cellulose-rich yucca fibers (80.25%, previous study) [11]. At a 5 wt% loading of the same yucca fiber category (PA11-YWR5), the tensile strength of the bio-composite significantly improved, reaching 34.75 ± 1.17 MPa. This enhancement reflects efficient load transfer, driven by the increased fiber content, which expands the interfacial area for stress distribution between the yucca fibers and the PA11 matrix [48]. Young's modulus surged by 28.81% to 1.27 ± 0.078 GPa, however, the larger standard deviation (SD) suggests localized fiber agglomeration, which can create stress concentrations and reduce reproducibility. Additionally, the elongation at break decreased to 30.17 ± 8.90%, a 20.90% reduction compared to the unreinforced PA11, aligning with the well-established restriction of polymer chain mobility and ductility in PA11 when rigid fibers are incorporated. This reduction in ductility reflects the fibers' limitation on the matrix's plastic deformation capacity [49].

Bio-composites containing traditionally extracted fibers (PA11-YT3 and PA11-YT5) exhibited enhanced interfacial consistency. Specifically, the PA11-YT3 variant exhibited a tensile strength of 34.64 ± 0.27 MPa, representing a minimal reduction of 0.55% compared to neat PA11, indicating that the fiber incorporation effectively maintains the material's strength. The Young's modulus increased significantly by 17.20%, reaching 1.15 ± 0.048 GPa, highlighting enhanced stiffness due to the reinforcing effect of the fibers [50]. The elongation at break was recorded at 30.83 ± 0.40%, a 19.12% reduction relative to pure PA11, consistent with the expected decrease in ductility caused by the restriction of polymer chain mobility upon incorporation of rigid fibers. The low standard deviation (SD) across these properties underscores uniform fiber dispersion and consistent interfacial bonding, minimizing stress concentrations and ensuring reliable mechanical performance. At a 5 wt% fiber loading (PA11-YT5), the bio-composite exhibited a tensile strength of 35.02 ± 0.29 MPa, marking a marginal improvement over neat PA11, indicative of enhanced load-bearing capacity due to effective fiber reinforcement. The Young's modulus increased significantly by 26.28%, reaching 1.24 ± 0.058 GPa, reflecting a substantial enhancement in stiffness attributed to the incorporation of traditionally extracted yucca fibers. This fiber loading remains within an optimal range, as it bolsters mechanical performance without introducing detrimental effects [51]. The elongation at break was measured at 34.89 ± 10.12%, representing an 8.50% reduction compared to pure PA11, consistent with the anticipated reduction in ductility due to restricted polymer chain mobility caused by the rigid fibers. The relatively stable tensile strength and low variability in the PA11-YT series underscore the efficacy of the traditional extraction process, which produces rough fibers compared to water-retted fibers. This results in improved mechanical interlocking and more uniform stress distribution across the fiber-matrix interface, enhancing overall composite performance [52].

A clear trend emerges when comparing the 3 wt% and 5 wt% fiber loadings for both extraction routes, increasing the fiber content consistently enhances the stiffness of the composites and, in most cases, maintains or slightly improves the tensile strength. This improvement is attributed to the larger volume fraction of load-bearing cellulose microfibrils, which increases the number of effective stresses-transfer pathways within the polymer matrix [53]. As more fibers are incorporated, their intrinsic rigidity contributes more significantly to the overall modulus, resulting in pronounced gains without evident penalties in strength [54,55]. Importantly, even at the highest investigated loading of 5 wt% yucca fibers, the composites did not exhibit any deterioration in mechanical performance. The tensile strength values remained comparable to or higher than those of neat PA11, and the increases in modulus were accompanied only by moderate, expected reductions in elongation, rather than indications of excessive brittleness or interfacial failure [56]. However, the incorporation of yucca fibers into PA11 leads to modest but consistent improvements in tensile propriety compared to neat PA11. While the increments are moderate due to the relatively low fiber contents (3 wt% and 5 wt%), they are sufficient to enhance the performance of semi-structural components. These results align with typical property thresholds required for automotive applications, indicating that even small enhancements can have practical significance [57].

Table 4 highlights the mechanical response of PA11 reinforced with diverse natural fibers, illustrating how fiber type and loading influence tensile strength and Young's modulus. The PA11-yucca composite (5 wt %) achieves a tensile strength of 35.02 MPa and a modulus of 1.24 GPa, demonstrating a favorable balance between stiffness and load-bearing capacity relative to low-content reinforcements such as wood or spinifex fibers. Notably, although jute fibers at high loading (20 wt%) exhibit a higher modulus (1.53 GPa), the corresponding tensile strength is reduced, emphasizing the critical interplay between fiber morphology, interfacial adhesion, and filler concentration [61]. These comparisons underscore the potential of yucca fibers as efficient reinforcements in PA11, providing comparable or superior mechanical performance at moderate loadings while leveraging the sustainability and renewable origin of the filler. This positions PA11-yucca systems as promising candidates for semi-structural applications where a balance of stiffness and tensile strength is required, without excessive filler content that could compromise processability or impact resistance.

3.3.2. *Flexural response of the bio-composite*

The flexural response of the fabricated bio-composites was characterized in accordance with ISO 178 using a three-point bending configuration, with the objective of elucidating the influence of dual-extracted yucca fibers on the stiffness and load-carrying capacity of the PA11 matrix. For each formulation, five specimens were tested to determine the flexural strength and flexural modulus, ensuring statistical reliability of the reported values. The resulting data, presented graphically in Fig. 7 and summarized numerically in Table 5, while a broader comparative positioning of the flexural performance relative to other PA11-based reinforced systems is provided in Table 6.

As presented in Table 5, all reinforced systems exhibited a noticeable improvement in flexural response compared with neat PA11, with the magnitude of the enhancement depending on both fiber content and extraction method. The unfilled PA11 matrix displayed a flexural strength of 41.81 ± 0.20 MPa and a modulus of 2.20 ± 0.13 GPa, which serves as the baseline for assessing reinforcement effects. Upon introducing 3 wt% of water-retted fibers (PA11-YWR3), a slight reduction in flexural strength was observed at 40.19 ± 0.64 MPa, which can be attributed to residual non-cellulosic layers and irregularities on the fiber surface resulting from the retting process [62]. These features are known to induce localized stress concentrations and to limit interfacial load transfer under bending conditions [63]. Despite this minor reduction in strength, the modulus increased to 2.26 ± 0.12 GPa, confirming the contribution of the rigid cellulose phase to stiffness even at low fiber content [64]. A further increase to 5 wt% water-retted fibers (PA11-YWR5) led to a recovery in flexural strength (41.84 ± 1.17 MPa) and a more pronounced enhancement in stiffness (2.45 ± 0.09 GPa). This improvement is consistent with the higher volume fraction of load-bearing fibers providing additional stress-transfer pathways and compensating for any interfacial heterogeneities.

In comparison, the bio-composites reinforced with traditionally extracted yucca fibers displayed superior flexural performance across all metrics. At 3 wt% (PA11-YT3), flexural strength reached 42.28 ± 0.66 MPa, coupled with a modulus of 2.65 ± 0.06 GPa. These results point to a cleaner fiber surface morphology and enhanced roughness produced by the traditional extraction, both of which favor improved interfacial adhesion and efficient load redistribution [65,66]. At 5 wt% (PA11-YT5), this trend is accentuated, with the flexural strength increasing to 43.08 ± 1.00 MPa and the modulus reaching 2.79 ± 0.05 GPa. The consistently low standard deviations (SD) reported for the PA11-YT series further confirm a more homogeneous fiber dispersion and a stable fiber-matrix interface.

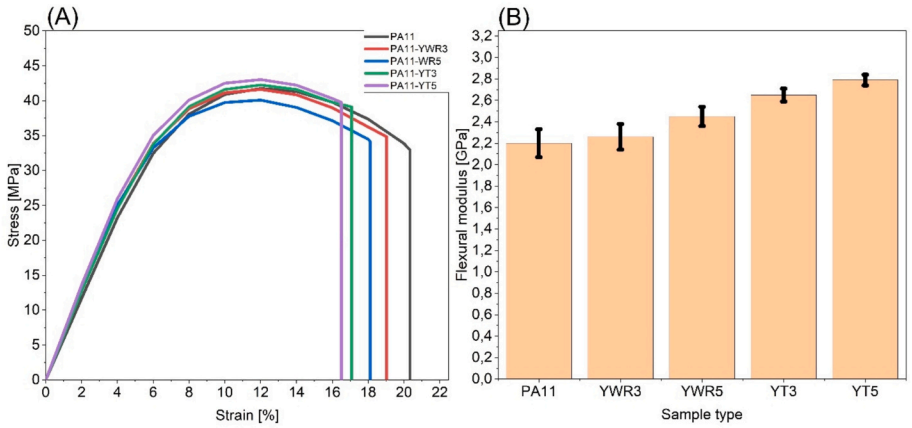

Fig. 7. Flexural response of neat PA11 and PA11/Yucca bio-composites. (A) Stress-strain curves. (B) Histogram of flexural modulus.

Table 5
Effect of yucca extraction method on bio-composites' flexural strength and stiffness.

Samples category	Flexural strength [MPa]		Flexural modulus [GPa]	
	Average	[SD]	Average	[SD]
Pure PA11	41.81	± 0.20	2.20	± 0.13
PA11-YWR3	40.19	± 0.64	2.26	± 0.12
PA11-YWR5	41.84	± 1.17	2.45	± 0.09
PA11-YT3	42.28	± 0.66	2.65	± 0.06
PA11-YT5	43.08	± 1.00	2.79	± 0.05

Table 6
Flexural property benchmark of PA11-based composites reinforced with natural and mineral fillers.

Matrix	Natural filler	Concentration [%]	Flexural strength [MPa]	Flexural modulus [GPa]	Reference
PA11	Yucca	5	43.08	2.79	This work
PA11	Bamboo	3	44.7	1.25	[67]
PA11	Basalt	10	79.00	2.51	[68]
PA11	Diatomaceous Earth	5	≈ 46	≈ 1.50	[69]

Table 6 situates the flexural response of the PA11-yucca composite within the broader landscape of PA11-based reinforced systems. At a low filler content of 5 wt%, yucca fibers enable a pronounced increase in flexural rigidity while maintaining a moderate flexural strength, indicative of an efficient stress-transfer mechanism under bending-dominated loading. Compared to other bio-based reinforcements, such as bamboo, the PA11-yucca system exhibits a significantly higher flexural modulus at comparable or lower filler levels, underscoring the intrinsic stiffness efficiency of yucca fibers. While mineral fillers like basalt achieve higher absolute flexural strength, this occurs at the expense of substantially higher filler content and increased material density. Notably, the flexural modulus attained by the yucca-reinforced composite approaches that of basalt-filled PA11 despite the large contrast in reinforcement nature and loading, highlighting the potential of yucca fibers as a lightweight, bio-derived alternative for stiffness-driven applications.

Taken together, these findings reveal that progressive fiber loading improves flexural stiffness while maintaining or slightly increasing strength, and that traditionally extracted fibers exhibit superior reinforcement efficiency compared to water-retted counterparts. Importantly, no evidence of over-reinforcement or adverse property trade-offs was observed at 5 wt%, suggesting that the composites remain well within an optimal reinforcement regime and that further increases in fiber content may be explored in future investigations without compromising structural integrity.

3.3.3. *Charpy impact resistance*

Understanding how natural reinforcements influence the fracture resistance of engineering polymers is central to designing next-generation bio-composites. Here, Charpy notched impact testing, was employed to capture the energy absorption and failure dynamics of PA11 reinforced with yucca fibers. The corresponding impact strength values are presented in Fig. 8, revealing the influence of fiber extraction route and content on the overall impact performance.

The Charpy impact results (Fig. 8) indicate a significant decline in impact resistance for all PA11-yucca composites compared to neat PA11, which exhibits the highest impact strength (8.78 $kJ{\cdot}m^{-2}$). The incorporation of yucca fibers constrains the matrix mobility and introduces rigid interfacial zones that serve as preferential sites for crack initiation, thereby reducing the overall toughness of the system [70]. Among the reinforced materials, the composites containing traditionally extracted fibers (PA11-YT3 and PA11-YT5) display superior impact performance relative to the water-retted ones (PA11-YWR3 and PA11-YWR5). The impact strength of the T3 and T5 PA11-composites reach 4.17 $kJ{\cdot}m^{-2}$ and 3.41 $kJ{\cdot}m^{-2}$, respectively, compared to 3.91 $kJ{\cdot}m^{-2}$ and 2.78 $kJ{\cdot}m^{-2}$ for the WR3 and WR5 systems. This enhancement reflects the stronger interfacial cohesion and more efficient stress transfer achieved with traditional fibers, which delay crack initiation and hinder its

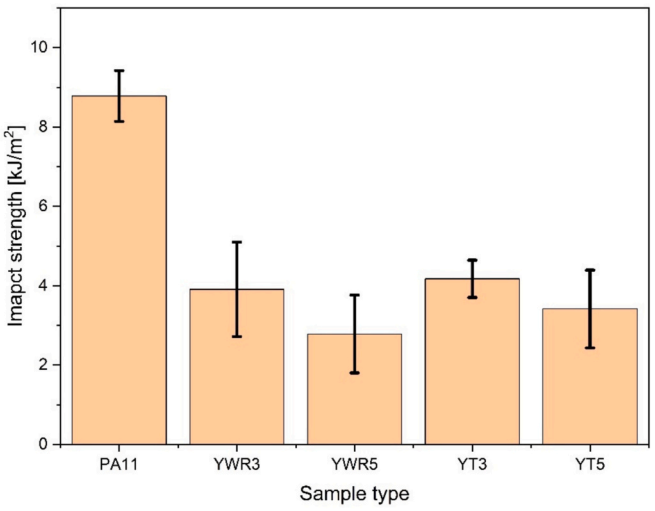

Fig. 8. Charpy impact strength of neat PA11 and yucca fiber-reinforced composites.

propagation across the interphase [71]. During impact, fracture energy is dissipated through fiber pull-out, matrix shear yielding, and crack deflection, mechanisms that operate more effectively when the interface remains well-bonded [72]. In contrast, the water-retted composites exhibit premature crack initiation and rapid propagation along weak interfacial regions. These poorly bonded zones act as stress concentrators, promoting interfacial debonding and unstable crack growth with limited plastic deformation [73]. The smoother and eroded surfaces of WR fibers, as observed by SEM, further confirm the brittle fracture mechanism governed by inadequate fiber-matrix adhesion. The overall decrease in impact strength across all fiber-reinforced systems stems from the restricted plastic deformation of the PA11 matrix, as the lignocellulosic inclusions act as rigid obstacles under dynamic loading [74]. While neat PA11 dissipates energy through matrix yielding and chain mobility, the presence of fibers shifts the failure mode toward a brittle, inter-facially dominated fracture [75].

Moreover, the fiber content plays a decisive role. Increasing the loading from 3 wt% to 5 wt% leads to a further reduction in impact strength, attributed to enhanced fiber-fiber interactions and local stress concentration [76]. At low contents, fibers contribute to crack deflection and energy dissipation, whereas at higher concentrations, fiber clustering and interfacial decohesion dominate, reducing the material's ability to absorb impact energy.

3.4. Heat deflection temperature of PA11/Yucca bio-composites

To further assess the thermo-mechanical stability of the developed bio-composites, heat deflection temperature (HDT) measurements were performed on neat PA11 and its yucca fiber-reinforced counterparts. This test provides a quantitative evaluation of the material's resistance at elevated temperature. Fig. 9 displays the variation in HDT values as a function of fiber content and extraction method.

The heat deflection temperature (HDT) results presented in Fig. 9, demonstrate a pronounced enhancement in the thermo-mechanical resistance of all PA11-yucca composites when compared to neat PA11. Specifically, the unreinforced matrix exhibits an HDT of 72.25 °C, whereas the incorporation of yucca fibers significantly elevates this value to 93.95 °C (T3%), 109.9 °C (T5%), 93.95 °C (WR3%), and 111.6 °C (WR5%). This marked improvement highlights the strong interfacial constraint that limits polymer chain mobility under simultaneous thermal and mechanical stresses [77]. The improvement of flexural modulus registered with the incorporation of yucca fibers is also responsible of the increment of the HDT that is carried in 3 point bending configuration (similarly to flexural test) at increasing temperature [78]. The increment in the HDT is thus correlated to the higher composite stiffness due to the presence of the fibers with the fiber that reduce the free volume in the systems; thus, enhancing the bio-composites thermal stability. The fibers, moreover, having higher thermal stability respect to the pure bio-PA11 matrix, improved the final thermal stability of the molded bio-composites. A closer inspection of the data reveals that traditionally extracted fibers (PA11-YT) lead to more consistent and cohesive interfacial behavior than their water-retted counterparts. The lower standard deviations (±0.92–3.39 °C) observed for PA11-YT3 and PA11-YT5 samples indicate a more uniform load transfer and stronger matrix-fiber adhesion, resulting in a stable thermal response across specimens. This finding aligns with the SEM observations, where PA11-YT-series composites exhibited cleaner, well-integrated interfaces without signs of interfacial voids or microcracking. In contrast, the PA11-YWR-series composites, though displaying slightly higher absolute HDT values at 5 wt% loading (111.6 °C), show greater variability (±4.60–3.82 °C), suggesting that water retting may induce surface irregularities or partial degradation of hemicellulose, thereby weakening the fiber-matrix coupling [79]. From a mechanistic standpoint, the enhanced HDT in the PA11-YT-series composites originates from the preservation of the native fibrillar order and waxy protective layers during traditional extraction [80]. These structural features enable a balanced interfacial adhesion, where the polymer chains are sufficiently anchored to delay flow under heat, yet not excessively degraded by chemical exposure [81]. Conversely, the aggressive conditions of water retting can lead to partial delamination of the fiber wall and localized stress accumulation, creating micro-defects that facilitate earlier onset of deflection under load. Furthermore, the increase in fiber content from 3 wt% to 5 wt% amplifies the HDT enhancement for both extraction routes, owing to the formation of thermally percolating fiber networks [82]. These networks restrict polymer chain relaxation and efficiently redistribute heat and mechanical stress. Similar percolation-driven reinforcement has been reported in pineapple leaf/high-density polyethylene (HDPE), where HDT improvements of up to 52% are associated with interphase densification and restricted amorphous mobility [83].

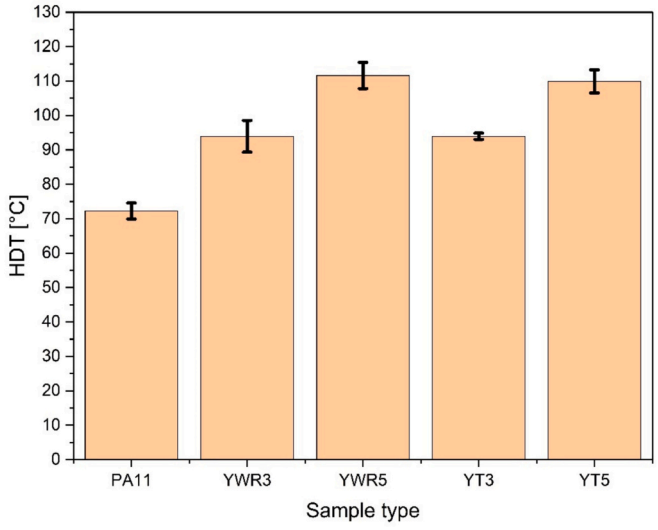

Fig. 9. Heat deflection temperature of PA11 and yucca fiber-reinforced bio-composites.

These results indicate that, the 55% increase in HDT relative to neat PA11 underscores the efficiency of yucca fibers as thermo-mechanical stabilizers. Yet, the superior interfacial cohesion and thermal reproducibility of the PA11-T composites highlight the advantage of traditional extraction in maintaining both fiber integrity and interfacial performance. Collectively, these findings position yucca-reinforced PA11 bio-composites as strong candidates for applications requiring dimensional and thermal stability, such as automotive components, electronic enclosures, and advanced structural systems exposed to demanding thermal environments.

3.5. DMTA results

The dynamic mechanical response of PA11 and its bio-composites reinforced with yucca fibers extracted through water retting (WR) and traditional (T) methods provides a quantitative fingerprint of the molecular and interfacial dynamics governing viscoelastic performance. The evolution of the storage modulus (E′) and loss factor (tan δ) reflects the interplay between fiber morphology, adhesion mechanisms, and polymer segmental mobility. The results, illustrated in Fig. 10 and summarized in Table 7, reveal significant enhancements in stiffness and viscoelastic performance.

The storage modulus (E'), which quantifies the material's ability to store elastic energy, was significantly enhanced in all bio-composites compared to neat PA11 across the tested temperature range. In the glassy state (−50 °C), the storage modulus of neat PA11 (1589 MPa) is significantly enhanced upon fiber incorporation, reaching 1837 MPa for PA11-YT5 and 1961 MPa for PA11-YWR5. Such an increase of around 15 and 24% aligns with the archetypal stiffening behavior observed in

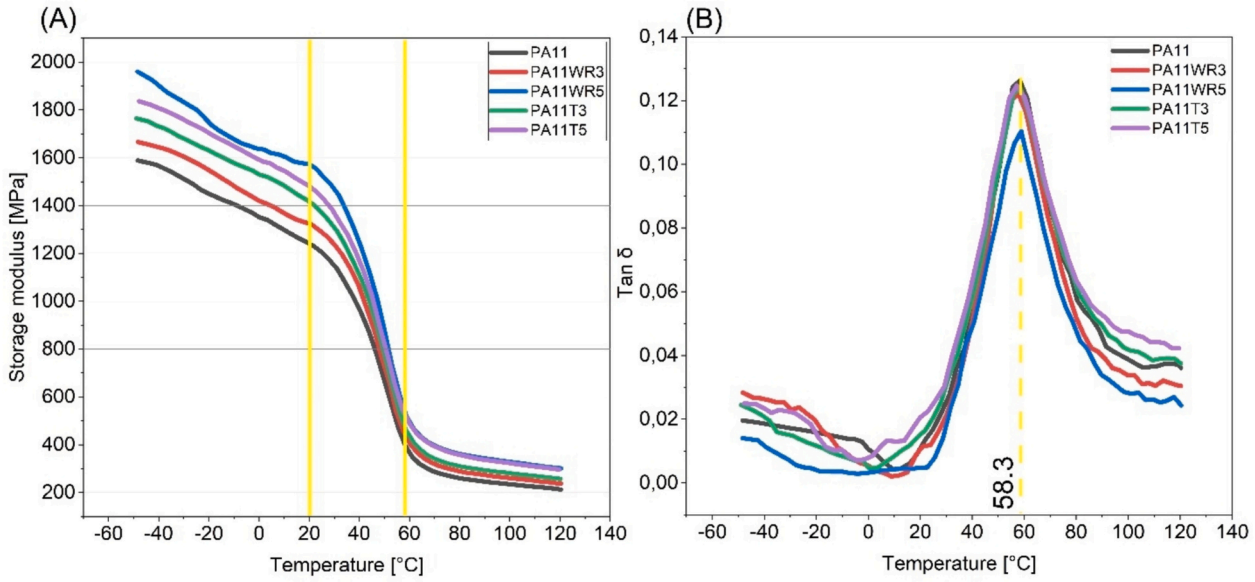

Fig. 10. Thermo-mechanical behavior of PA11 and yucca fiber bio-composites revealed by DMA. (A) storage modulus evolution and (B) molecular relaxation transitions (tan δ).

Table 7
Dynamic mechanical properties of PA11 and PA11 yucca fiber bio-composites. (E'_{glass}/E'_{rubber} (E' at °25C / E' at Tg) is stiffness retention ratio.)

Sample type	E' at −50 °C [MPa]	E' at 20 °C [MPa]	E' at Tg [MPa]	$\frac{E'_{glass}}{E'_{rubber}}$	Tg [°C]	Tan δ max
PA11	1589	1231	396.2	3.10	58.3	0.126
PA11-YWR3	1666	1321	453.6	2.91	57.7	0.122
PA11-YWR5	1961	1575	517.9	3.04	58.8	0.110
PA11-YT3	1764	1425	460.3	3.09	58.6	0.123
PA11-YT5	1837	1482	549.2	2.69	57.1	0.124

biopolyamide-based composites, where the rigid inclusions act as micro-anchors restricting chain displacement [84]. Notably, this superior stiffness at sub-zero temperatures suggests that yucca-reinforced PA11 remains mechanically robust in extreme cold environments (snow regions, polar climates), making these materials particularly attractive for automotive applications operating in low-temperature climates, where polymer brittleness typically increases. However, the magnitude and temperature dependence of E′ reveal more subtle effects of interfacial cohesion [85]. Despite PA11-YWR5 exhibiting the highest absolute modulus, the PA11-YT series maintains superior interfacial continuity and stress transfer stability as temperature increases, indicating that the micro-mechanical bonding in PA11-YT composites is more resilient against thermal relaxation. The rougher topography of fibers extracted by the traditional method, observed in SEM analysis (Section 3.1), enhances mechanical interlocking and adhesive wetting, forming a network of polymer-fiber bridges that efficiently transmit stress. This interlocking mechanism creates localized regions of strain hardening, delaying viscoelastic relaxation and minimizing shear slip at the interface [86]. As the system approaches the α-transition, the influence of interfacial cohesion becomes dominant [87]. The modulus retention at 20 °C (PA11-YT5: 1482 MPa vs PA11-YWR5: 1575 MPa) and the higher E′ at Tg for PA11-YT5 composites (up to 549 MPa) indicate that the traditional method fibers promote a percolating stress-transfer network capable of restraining the cooperative motion of polymer chains [88]. This behavior evidences the presence of a rigid amorphous interphase (RAI), where amorphous chains adjacent to the fiber surface lose configurational freedom due to hydrogen bonding and mechanical confinement [89].

In addition, the stiffness retention ratio (E'_{glass}/E'_{rubber}), spanning 2.7–3.1, is characteristic of partially constrained semi-crystalline polymers, in agreement with values reported in literature [90]. Ratios exceeding 2.5 suggest a well-developed interphase with efficient energy storage and minimal chain slippage, a hallmark of strong interfacial adhesion. In the PA11-YT system, this ratio reflects the synergy between physical anchoring and interfacial entanglement of polymer chains, where topological restrictions propagate several nanometers into the amorphous matrix, effectively reinforcing the macroscopic viscoelastic response [91]. Furthermore, the glass transition temperature (Tg) remains nearly invariant (57–59 °C) across all formulations, highlighting that the fibers act as rigid inclusions rather than plasticizers [92]. The lack of Tg shift, coupled with higher E′ retention, supports the rigid amorphous fraction model, wherein the interphase immobilizes amorphous chains without altering the fundamental α-relaxation dynamics [93]. Finally, the tanδ spectra exhibit a single, symmetric α-relaxation peak near 57–59 °C for all composites, confirming the absence of phase segregation and validating the homogeneous dispersion of yucca fibers within the PA11 matrix [94]. The slight reduction in $\tan\delta_{max}$ (from 0.126 for PA11 to 0.124 for PA11-YT5) indicates lower internal friction and reduced free-volume mobility, both consequences of constrained molecular motion at the interface.

3.6. Functional response of PA11 bio-composites under moisture exposure

3.6.1. Water absorption kinetics and diffusion behavior

To evaluate the hydrothermal stability of the developed systems, water absorption tests were carried out at 37 °C and 85% RH for 15 days. Fig. 11 presents the sorption kinetics, while Table 8 summarizes the equilibrium uptake (M∞) and apparent diffusion coefficients (D_{app}) derived from Fick's model. This analysis provides direct insight into the molecular transport phenomena and interfacial resistance governing moisture diffusion in PA11-yucca composites.

The evolution of water absorption for PA11 and its yucca fiber-reinforced composites over 15 days under controlled hygrothermal conditions provides critical insight into the interplay between polymer polarity, fiber hydrophilicity, and interfacial morphology. As shown in

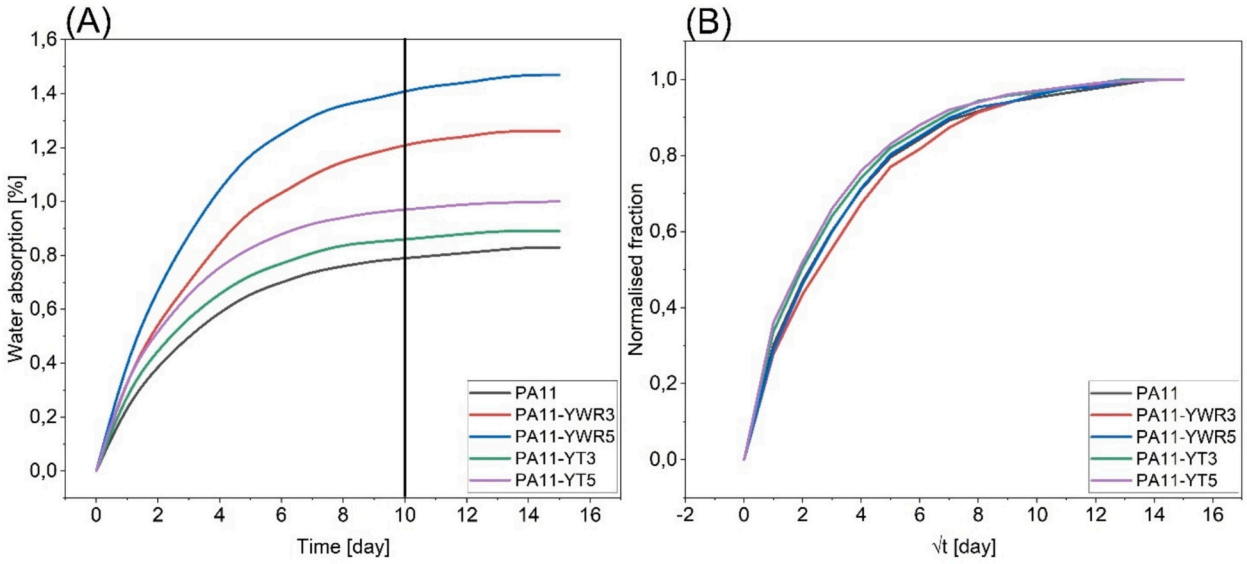

Fig. 11. - Water absorption behavior of composites. (A) Water absorption kinetics of PA11 and PA11-yucca bio-composites. (B) Fickian diffusion plots for the corresponding systems.

Table 8
Equilibrium water uptake and apparent diffusion coefficients of PA11 and PA11-yucca bio-composites.

Sample type	Water absorption, M_∞ [%]	D_{app} [$m^2.s^{-1}$]
Neat PA11	0.83	9.28×10^{-13}
PA11-YWR3	1.26	7.93×10^{-13}
PA11-YWR5	1.47	8.87×10^{-13}
PA11-YT3	0.89	1.09×10^{-13}
PA11-YT5	1.00	1.18×10^{-13}

Fig. 6A, all materials exhibit a two-stage sorption profile typical of Fickian-type diffusion: a fast initial uptake (up to 70% of the total gain within the first 3 days), followed by a gradual deceleration as the system approaches equilibrium after approximately 10–12 days. This behavior arises from the coupling of molecular diffusion through the polymer's amorphous domains and relaxation-driven transport along the fiber-matrix interfaces [95]. In this context, neat PA11 demonstrates the lowest equilibrium moisture uptake (around 0.83%), reflecting the semi-crystalline character and long methylene segments that reduce water affinity compared to shorter-chain polyamides such as PA6 [96]. Upon incorporation of yucca fibers, the equilibrium moisture content increases significantly, in line with the intrinsic hydrophilicity of lignocellulosic reinforcements and the introduction of capillary microchannels along the interfaces [97]. A key distinction emerges between composites containing water-retted (WR) and traditionally extracted (T) fibers. Despite the slightly higher cellulose exposure of WR fibers, the composites PA11-T3 and PA11-T5 show lower overall water absorption (0.89–1.00%) than their WR counterparts (1.26–1.47%). This counterintuitive result can be rationalized by considering the superior interfacial cohesion for the PA11-YT composites, which limits the penetration of moisture through the interfacial zone [98]. In addition, the effect of fiber loading further modulates the moisture uptake. Increasing the fiber fraction from 3 wt% to 5 wt% amplifies the absorbed moisture by approximately 12%, a trend attributed to the greater interfacial area and the percolation of hygroscopic pathways within the matrix.

As shown in Table 8, the apparent diffusion coefficients (D_{app}) further highlight the influence of fiber extraction method and interfacial morphology on water transport kinetics. Although all materials exhibit Fickian-type diffusion, the magnitude of D_{app} varies by almost one order of magnitude across the different systems. The neat PA11 shows a moderate diffusion rate (9.28×10^{-13} $m^2.s^{-1}$), governed by its amorphous phase fraction. Incorporation of WR fibers into PA11 matrix slightly reduces D_{app} to approximately 8×10^{-13} $m^2.s^{-1}$, suggesting that water diffusion proceeds mainly through hydrophilic pathways within the fiber lumen and imperfect interfacial contacts [99]. In contrast, composites reinforced with traditionally extracted fibers display much lower diffusion coefficients, close to 1×10^{-13} $m^2.s^{-1}$, indicating a markedly slower diffusion process. This is consistent with the superior interfacial adhesion and reduced voids, which effectively block capillary water migration [100]. The diffusion kinetics thus confirm that fiber-matrix interfacial integrity dominates the moisture transport behavior, more than fiber hydrophilicity alone [101].

3.6.2. *Effect of humidity exposure on the load-bearing capacity*

Following exposure to a controlled hygrothermal environment of 85% relative humidity (RH) at 38 °C for 30 days, the tensile mechanical properties of polyamide 11 (PA11)-based bio-composites were meticulously characterized. The results, detailed in Table 9, encompass the mean values and associated standard deviations of tensile strength, Young's modulus, and elongation at break, alongside their relative variations (Δ) with respect to the baseline properties measured in the anhydrous state.

For the reference material, neat PA11, the tensile strength and Young's modulus decreased only marginally (less than 1%), indicating the relatively stable microstructure of the unreinforced matrix under humid conditions. These results confirm also the good resistance of bio-PA11 to humidity exposure, thanks to the presence of fewer hydrogen bonds, respect to PA6 and PA66 fossil-base counterparts [102]. The negligible reduction in elongation at break (0.32%) further confirms that the inherent ductility of PA11 is largely retained after moisture absorption. These minimal variations highlight the excellent hygrothermal stability of pristine PA11 and its low susceptibility to moisture-induced degradation under the tested conditions [39]. Conversely, bio-composites incorporating YWR and YT reinforcements manifested distinct mechanical responses, modulated by the reinforcement type and loading fraction. In the PA11-YWR composites, the presence of water-retted fibers introduced additional interfacial phenomena. At 3 wt% fiber loading, tensile strength declined by only 0.72%, indicating that the overall load-bearing capacity was not drastically affected. However, the elongation at break exhibited a sharp decrease of over 50%. This can

Table 9
Tensile performance of PA11-based bio-composites after moisture conditioning. (Relative variation "Δ" is reported with respect to dry-state properties).

Samples category	Tensile strength		Young's modulus		Elongation	
	Average ± SD [MPa]	Δ*TS* [%]	Average ± SD [GPa]	Δ*E* [%]	Average ± SD [%]	Δε [%]
Pure PA11	34.60 ± 0.20	↓ 0.67	0.97 ± 0.006	↓ 0.98	38.01 ± 3.10	↓ 0.32
PA11-YWR3	33.39 ± 0.54	↓ 0.72	1.11 ± 0.026	↓1.08	17.07 ± 0.55	↓ 52.44
PA11-YWR5	34.15 ± 2.14	↓ 1.74	1.09 ± 0.057	↓ 13.4	16.48 ± 2.10	↓ 45.37
PA11-YT3	34.00 ± 0.63	↓ 1.84	1.01 ± 0.075	↓11.7	19.04 ± 0.64	↓ 38.25
PA11-YT5	34.35 ± 0.76	↓ 1.92	1.12 ± 0.098	↓ 9.68	16.58 ± 1.44	↓ 52.47

be attributed to the smoother surface morphology of water-retted fibers, which inherently offers fewer asperities and micro-anchoring sites [103]. When moisture diffuses along the interface, these smoother fibers tend to form micro-gaps or weak interfacial zones, reducing the ability of the composite to deform plastically without initiating interfacial debonding or microcracks [104]. At 5 wt% concentration, the trend was similar, with tensile strength decreasing by 1.74%. The Young's modulus, however, dropped by 13.4%, a more pronounced decline than at 3 wt%. This stronger reduction is likely linked to increased fiber-fiber interactions at higher loading, which can hinder efficient matrix infiltration and create micro-void networks that are more sensitive to humidity [105]. The 45.37% reduction in elongation further reflects the formation of a more rigid but less compliant microstructure.

Conversely, the composites reinforced with traditionally extracted fibers (PA11-YT series) exhibited a different response profile. At 3 wt% loading, tensile strength decreased by 1.84% and the modulus by 11.7%. Although this reflects a certain susceptibility to humidity-induced softening, the SEM observations from earlier analysis suggest that the rougher surface and porosity of YT fibers enhance mechanical interlocking and provide additional pathways for matrix penetration, which helps preserve tensile integrity under humid conditions [106]. Nevertheless, swelling of the natural fibers and the diffusion of water into their lumen can lead to local stresses at the interface, explaining the significant reduction in elongation (38.25%). At 5 wt% (PA11-YT5), tensile strength showed a 1.92% decrease, and modulus declined by 9.68%, which is slightly less than the reduction observed for PA11-YWR5. This suggests that the interfacial architecture created by traditional extraction remains more resilient to moisture ingress. The elongation, however, still dropped by more than 50%, consistent with restricted chain mobility in a fiber-rich matrix and the onset of micro-defects at the interface [107].

Taken together, these findings underscore the intrinsic capacity of PA11-yucca bio-composites to withstand prolonged humidity exposure while retaining the integrity of their internal architecture. Rather than compromising the material, the moisture-induced changes remain moderate and manageable, indicating that these formulations are well suited for applications where environmental fluctuations are unavoidable. Future investigations could focus on long-term cyclic humidity testing or accelerated aging protocols to further validate their performance envelope and support their adoption in industrial environments such as automotive interiors, where lightweight, bio-sourced materials with reliable durability are increasingly in demand.

3.6.3. Environmental humidity effects on flexural performance

To assess the long-term mechanical stability of the developed bio-composites under humid and thermal stress, flexural tests were conducted after hydrothermal aging for 30 days. This environment was selected to simulate realistic service conditions for polyamide-based materials, where water absorption and molecular relaxation can progressively compromise the structural integrity. In this context, the corresponding flexural mechanical prosperities are summarized in Table 10.

After 30 days of conditioning at 38 ± 0.5 °C and 85 ± 1% relative humidity, all samples exhibited a clear decrease in both flexural strength and modulus compared to their initial values, confirming the sensitivity

Table 10
Impact of moisture exposure on the flexural response. (Relative variation "Δ" is reported with respect to dry-state properties).

Sample type	Flexural strength		Flexural modulus	
	Average ± SD [MPa]	ΔFS [%]	Average ± SD [MPa]	ΔFM [%]
Pure PA11	32.88 ± 1.28	↓ 21.35	1476.92 ± 71.41	↓ 32.91
PA11-YWR3	32.86 ± 0.47	↓ 18.25	1481.12 ± 39.73	↓ 34.46
PA11-YWR5	33.67 ± 0.75	↓ 19.15	1545.32 ± 39.38	↓ 37.08
PA11-YT3	33.82 ± 0.76	↓ 20.00	1562.67 ± 44.35	↓ 40.92
PA11-YT5	38.60 ± 2.40	↓ 10.40	1725.26 ± 66.94	↓ 38.17

of PA11-based systems to hydrothermal environments. However, the extent of degradation strongly depended on the fiber type and content. The neat PA11 experienced a significant reduction of approximately 21.35% in flexural strength and 32.91% in modulus, highlighting the pronounced plasticization of the polyamide matrix under moisture uptake, which induces chain mobility, hydrogen bond disruption, and micro-void formation. These effects are consistent with the well-documented hydrolytic instability of polyamides reported in literature [108]. Interestingly, the incorporation of yucca fibers, even at low loadings (3–5 wt%), mitigated the loss of mechanical integrity. For the water-retted fiber composites (PA11-YWR3 and PA11-YWR5), the flexural strength decreased by only ~18–19%, while the modulus showed a modest reduction (around 34–37%). This behavior suggests that the fibrous reinforcement acted as a stress-transfer skeleton, limiting the polymer's dimensional relaxation during the hygroscopic swelling stage [109]. The limited hydrophilicity of WR fibers and their moderate aspect ratio may have balanced water uptake and stress redistribution. In contrast, composites reinforced with traditionally extracted fibers composites (PA11-YT5) demonstrated a superior resistance to hydrothermal degradation. The PA11-YT5 category exhibited the highest post-aging flexural strength (38.60 MPa) and modulus (1725 MPa), with the lowest strength decrease (around 10%) among all formulations. This enhancement can be attributed to the denser microstructural cohesion and higher fiber stiffness provided by the traditional extraction route, which tends to preserve the intrinsic cellulose crystallinity and reduce hemicellulose remnants, factors known to improve dimensional stability during moisture exposure [110].

The distinction between WR and T composites reflects how the extraction method governs the fiber's supramolecular organization and interfacial durability under moisture exposure. Water-retted fibers, with more amorphous constituents, tend to absorb and transport water more readily, facilitating localized swelling and stress relaxation [111]. Conversely, traditionally extracted fibers create a denser interphase with better load transfer and dimensional stability, leading to enhanced retention of stiffness. These findings align with previous reports on natural-fiber-reinforced polyamides, where interfacial integrity and fiber hydrophobicity were identified as key determinants of long-term mechanical durability [112,113].

A clear positive correlation between fiber loading and property retention was also observed: both PA11-YWR and PA11-YT composites

at 5 wt% exhibited higher post-aging stiffness than their 3 wt% counterparts. This trend supports diffusion-relaxation coupling models, wherein rigid inclusions constrain the local swelling of amorphous polymer regions, thereby delaying microcrack propagation and mechanical softening [114]. The cooperative interaction between PA11 chains and the lignocellulosic phase likely forms a semi-interpenetrating hydrogen-bonded network that stabilizes the amorphous fraction during hydrothermal aging.

3.7. Cradle-to-gate environmental signatures of PA11 bio-composites

To complement the mechanical and thermal analyses, a life cycle and economic assessment was carried out to evaluate the sustainability of the PA11-yucca bio-composites. This cradle-to-gate approach covers fiber extraction, grinding, and composite fabrication, linking material processing to both environmental and economic performance. Table 11 summarizes the global warming potential (GWP) and cost distribution for neat PA11 and its fiber-reinforced counterparts.

The cradle-to-gate environmental and economic profiles of the PA11-yucca fiber composites are summarized in Table 11. As expected, the neat PA11 matrix exhibited a global warming potential (GWP) of 1.30 kg CO_2 eq./kg, aligning with the carbon footprint typically reported for bio-based polyamides derived from castor oil. This footprint is markedly lower than that of conventional fossil-based polyamides, such as PA6 (≈9.1 kg CO_2 eq./kg) and PA12 (≈6.9 kg CO_2 eq./kg), highlighting the substantial environmental advantage of PA11. Even polypropylene, despite its dominant role in the automotive sector due to its low cost and high manufacturability, still carries a higher impact at around 1.6 kg CO_2 eq./kg, underscoring the exceptional carbon efficiency offered by PA11-based systems [115]. Upon fiber incorporation, a systematic reduction in total GWP was observed across all bio-composite formulations, reaching values of approximately 1.27–1.29 kg CO_2 eq./kg. While the absolute reduction appears modest, it reflects a tangible mitigation effect associated with the partial substitution of the polymeric phase by a renewable, low-emission filler, a critical step toward achieving net-zero carbon materials [116]. This trend becomes particularly meaningful when contextualized within the life-cycle perspective of high-performance polymers. The yucca fibers act as carbon sinks, temporarily storing biogenic carbon absorbed during plant growth [117]. Even at low loadings (3–5 wt%), this renewable contribution partially offsets the embedded emissions of PA11, underscoring the disproportionate environmental leverage of natural fillers in advanced polymer systems. The fiber-related impact, comprising extraction step (0.6–0.8 kg CO_2 eq./kg) and grinding step (0.22 kg CO_2 eq./kg), remains marginal due to the mild extraction conditions and localized processing, confirming that bio-filler integration can be environmentally favorable without relying on energy-intensive steps [118]. Comparing both extraction routes, the water-retted yucca fibers (YWR) slightly outperformed their traditional extracted counterparts (YT) in terms of GWP, emphasizing that fiber extraction method is a decisive parameter in determining the true sustainability of the final composite. Traditional extracted fibers, while beneficial for mechanical interfacial compatibility, introduces additional energy demand (energy intensity of the thermal step in the extraction technique) that modestly increases the embodied carbon. Such trade-offs illustrate the multi-objective optimization challenge in bio-composite design, where performance gains must be balanced with energy and emission efficiency [119].

Table 11
Cradle-to-Gate global warming potential (GWP) and cost analysis of PA11-yucca fiber bio-composites.

Sample type	Pure PA11	PA11-YWR3	PA11-YWR5	PA11-YT3	PA11-YT5
Matrix GWP [kg CO_2 eq./kg]	1.30	1.30	1.30	1.30	1.30
Matrix percentage [%]	100	97	95	97	95
Total matrix GWP [kg CO_2 eq./kg]	1.30	1.261	1.235	1.261	1.235
Fiber extraction [kg CO_2 eq./kg]	–	0.6	0.6	0.8	0.8
Fiber grinding [kg CO_2 eq./kg]	–	0.22	0.22	0.22	0.22
Fiber concentration [%]	–	3	5	3	5
Total fiber GWP [kg CO_2 eq./kg]	–	0.024	0.041	0.030	0.056
Total bio-composite GWP [kg CO_2 eq./kg]	1.30	≈1.28	≈1.27	≈1.29	≈1.28
Matrix cost [€/kg]	9	8.73	8.55	8.73	8.55
Fiber powder cost [€/kg]	–	0.12	0.20	0.09	0.15
Total composite cos [€/kg]	9	8.85	8.75	8.82	8.70

From an economic standpoint, a consistent downward trend in the overall material cost was observed upon fiber incorporation. The unit cost decreased from 9 €/kg for neat PA11 to approximately 8.7–8.8 €/kg for the bio-composites, primarily due to partial polymer substitution and the low market price of yucca powders (3–4 €/kg, including grinding, electricity, and transport). This substitution effect highlights the intrinsic cost-leverage potential of natural fillers, where even small loadings can induce tangible reductions in the overall production cost [120]. More importantly, this cost mitigation aligns with the environmental advantages observed in the life-cycle assessment, illustrating that economic competitiveness and ecological performance can converge within the same design space, a synergy still rarely realized in sustainable polymer engineering. The cost structure remained relatively stable across the two fiber types, indicating that the economic viability of fiber-reinforced PA11 systems is largely insensitive to extraction routes at low filler fractions. Such stability underscores the scalability potential of this approach for industrial implementation, particularly in sectors where feedstock cost and embodied energy dominate the material footprint [121]. When compared with other bio-based reinforcements reported in the literature, the yucca-reinforced PA11 system emerges as a cost-efficient and technically robust alternative [122].

Beyond quantitative metrics, these findings carry broader implications. The PA11-yucca system exemplifies the next generation of eco-functional composites, where biogenic fillers not only enhance stiffness and reduce polymer dependency but also contribute to lowering the cradle-to-gate carbon intensity [123]. The marginal gains per kilogram become exponentially significant when extrapolated to large-scale production, especially in automotive, consumer goods, and additive manufacturing sectors increasingly governed by carbon budgets. In this context, the present study provides a quantitative validation of bio-reinforcement as an effective decarbonization pathway for engineering polymers. The synergy between PA11's bio-origin and yucca's renewability demonstrate that sustainability and performance are not antithetical but mutually reinforcing design objectives. When integrated into circular life-cycle strategies, such as reprocessing, fiber recovery, or bio-based matrix recycling, these composites could serve as a blueprint for low-carbon polymeric materials, establishing a scalable model for the transition toward carbon-resilient and economically accessible bio-composites [124,125].

4. Industrial prospects and green application pathways

The pursuit of sustainability in the automotive industry is not merely a shift in material selection, it represents a profound rethinking of how performance, processability, and planetary responsibility can coexist within a unified design philosophy. In this vision, the PA11-yucca bio-composites developed in this work stand as archetypes of the next generation of engineering materials: bio-derived, structurally competent, and industrially scalable. Fig. 12 provides an overview of the key benefits and potential applications of such bio-composites in automotive

Fig. 12. Key benefits and potential applications of bio-composites in the automotive industry.

manufacturing.

To begin with, the experimental results obtained in this study demonstrate that the developed PA11-yucca bio-composites maintain their mechanical integrity and thermal stability even after exposure to controlled humidity aging, with only marginal variations in tensile, flexural, and impact responses. This resilience under humid conditions, uncommon among many bio-based composites, highlights a key advantage for automotive use, where materials are often exposed to fluctuating environmental conditions. In particular, the high mechanical performance recorded for PA11-YT5%, both before and after moisture conditioning, confirms its suitability for semi-structural interior components that must sustain bending and tensile loads while resisting degradation over time. Furthermore, beyond their mechanical robustness, the thermal behavior of the composites remained stable, with no significant shifts in softening or degradation profiles. This indicates that the incorporation of yucca fibers does not compromise the thermal processing window. Such stability is essential for applications in the automotive sector, where components experience variable service temperatures and require reliable performance throughout the vehicle's lifespan [126]. The combination of humidity resistance and thermal stability therefore positions these bio-composites as viable alternatives to conventional glass-fiber-reinforced plastics. From an application perspective, these materials are ideally suited for semi-structural and interior automotive parts (Fig. 12), including door panels, dashboard substrates, trunk liners, seat backs, underbody shields, and engine covers. Their combination of enhanced stiffness, thermal stability, and environmental durability enables significant lightweighting and sustainability benefits for everyday automotive use. Beyond conventional cars, the exceptional thermo-mechanical performance of traditionally extracted composites positions them as promising candidates for high-performance vehicles and motorsports applications, including Formula 1 and other racing platforms, where extreme loads, elevated temperatures, and precise dimensional stability are critical. This dual focus highlights the versatility of yucca-reinforced PA11 bio-composites across the automotive spectrum, from mainstream mobility solutions to cutting-edge high-performance engineering. More specifically, based on the measured tensile strength (35.02 MPa), flexural modulus (43.08 GPa), and impact resistance (3.41 $kJ \cdot m^{-2}$) of the PA11-YT5 composite, this material is ideally suited for center consoles. These components primarily experience bending and static loads, where dimensional stability and stiffness are essential, but high impact resistance is not critical. The combination of thermal stability, fiber-matrix cohesion, and adequate mechanical performance ensures reliable long-term service while leveraging the sustainable, bio-based nature of the composite.

The advantages of integrating natural-fiber composites into the automotive sector are already well-documented. Published paper demonstrate that substituting miscanthus fiber in polypropylene matrix can reduce component weight by 13.4%, lower energy consumption, and cut cradle-to-gate CO_2 emissions by up to 1.63 kg CO_2 eq per kilogram of material [127]. The PA11-yucca systems developed herein extend these benefits further: being derived from renewable castor oil and plant-based fibers, their total carbon footprint is reduced to approximately 1.27 kg CO_2 eq/kg. This footprint reduction, coupled with around 10% cost saving, positions these materials as highly competitive candidates for eco-certified automotive platforms. Beyond the classical metrics of strength and sustainability, PA11-yucca bio-composites exhibit additional functionalities of industrial relevance. Their lower abrasiveness toward tooling extends mold life and reduces maintenance frequency, thereby minimizing production downtime and overall manufacturing costs. The possibility of partial recyclability and the potential for biodegradation at end-of-life stages align perfectly with circular economy models, particularly in the context of ISO 14040-compliant life cycle assessment (LCA) frameworks increasingly adopted by major automotive manufacturers [128,129]. From an engineering standpoint, the PA11-yucca composites also demonstrate design flexibility. Through controlled fiber content, filler size, or hybridization with other biogenic fillers, tailored mechanical responses can be achieved, paving the way for multi-functional automotive parts that combine mechanical strength, and aesthetic quality. Moreover, given the excellent adhesion observed under SEM analysis and the high crystallinity stability detected by DSC, these materials could be further optimized for injection-compression molding, 3D-printed reinforcement structures, or multi-material over-molding, technologies currently driving innovation in sustainable lightweight design.

Ultimately, this study illustrates that green performance materials (GPM) are not a compromise, but an advancement. The PA11-yucca systems epitomize the synergy between renewable chemistry and structural engineering, establishing a new design philosophy where materials are conceived not only for their strength and durability but also for their ecological intelligence [130]. Their adoption in the automotive sector could mark a transformative milestone, redefining how sustainability is measured, not as an environmental constraint, but as a vector of innovation and competitiveness.

5. Conclusion

The transition from conventional polymers to high-performance bio-based composites represents more than a technological step, it marks a paradigm shift toward sustainable material intelligence. This work introduces dual-extracted yucca fiber-reinforced PA11 as a pioneering pathway for designing renewable, resilient, and industrially scalable composites through injection molding. By integrating yucca fibers obtained via two distinct extraction routes into a bio-based PA11 matrix, this study unveils a new class of sustainable composites that combine mechanical robustness with environmental responsibility. Through the coupling of renewable reinforcement and a scalable polymer system, it transcends the traditional trade-off between strength, stiffness, and eco-efficiency. The key outcomes of this research can be summarized as follows:

- SEM analysis revealed distinct interfacial morphologies between the two extraction routes, water-retted fibers exhibited smooth surfaces that led to minor micro-voids, whereas traditionally extracted fibers displayed a rough and porous texture, enabling full matrix impregnation, strong adhesion, and efficient load transfer.

- Mechanical excellence was achieved by the traditionally extracted series (PA11-T5), which reached tensile and flexural strengths of 35.02 MPa and 43.08 MPa, clearly outperforming neat PA11.
- Water-retted systems (PA11-WR5) demonstrated balanced mechanical behavior, combining strength and ductility with remarkable impact toughness and a high heat deflection temperature of 111.6 °C.
- DMA results confirmed enhanced stiffness retention across the temperature range, with storage moduli above 1800 MPa at −50 °C and 1480 MPa at 20 °C for PA11-YT5, alongside stable glass transitions near 58 °C, evidence of strong interfacial interlocking and restricted chain mobility.
- Moisture absorption remained below 1.5%, with lower diffusion coefficients for traditionally extracted fibers, indicating superior interfacial cohesion and barrier efficiency.
- Both composite systems preserved over 80% of their mechanical integrity under hygrothermal aging (37 °C, 85% RH, 30 days), confirming excellent durability.
- Life cycle assessment revealed a meaningful environmental advantage, reducing the global warming potential by approximately 1.27 kg CO_2 eq/kg and lowering overall processing costs compared to neat PA11.

Collectively, these findings define a new generation of bio-based composites that unite strength, resilience, and sustainability. The injection-molded PA11/yucca systems demonstrate that natural reinforcements can reach industrial-grade performance while minimizing ecological impact, paving the way for next-generation lightweight materials in automotive and structural applications. Beyond performance, this study exemplifies how nature-inspired design can guide the next era of sustainable material evolution. Hardness was not included in the current study because it primarily reflects surface resistance, whereas the selected tensile, flexural, and impact tests provide a more representative assessment of the composite's bulk mechanical performance and fiber-matrix interactions. However, hardness measurements will be systematically included in future work to complement these results. While the comparison between the two fiber extraction methods showed only moderate differences in mechanical, thermal, and crystallization properties, this baseline assessment provides valuable insights into the influence of extraction routes on fiber characteristics and composite behavior. Future work will focus on chemical modifications (alkali treatment) of the fibers to further enhance performance and establish stronger structure-property relationships. Future perspectives also include the exploration of different fiber contents to optimize the balance between reinforcement level and mechanical performance. In addition, developing and testing a real automotive prototype component will serve as a crucial step toward validating the industrial applicability of these sustainable bio-based composites.

CRediT authorship contribution statement

Mohamed Amine Kacem: Writing – review & editing, Writing – original draft, Visualization, Validation, Software, Methodology, Investigation, Formal analysis, Data curation, Conceptualization. **Laura Aliotta:** Writing – review & editing, Methodology, Investigation, Formal analysis, Data curation, Resources. **Vito Gigante:** Writing – review & editing, Supervision, Methodology, Investigation. **Nassila Sabba:** Writing – review & editing, Supervision, Methodology, Investigation. **Sylvie Masse:** Writing – review & editing, Supervision, Methodology, Investigation. **Mahdi Bodaghi:** Writing – review & editing, Supervision, Resources, Project administration, Methodology, Investigation, Conceptualization, Visualization.

Declaration of competing interest

The authors declare that they have no known competing financial interests or personal relationships that could have appeared to influence the work reported in this paper.

Acknowledgements

This work was partially supported by the Engineering and Physical Sciences Research Council (EPSRC) Innovation Launchpad Network+Researcher in Residence scheme [grant numbers: EP/W037009/1, EP/X528493/1, project: RIR26C230615-6]. The authors would also like to express their gratitude to the University of Pisa for their support and valuable collaboration throughout this work.

Data availability

Data will be made available on request.

References

[1] R. Benamrane, M.S. Bennouna, M. Fellah, K. Sadek, The improvement of the tensile properties of alfa fibers using the Taguchi method, Ind. Crop. Prod. 221 (2024) 119398.
[2] S. Awad, R. Siakeng, E.M. Khalaf, M.H. Mahmoud, H. Fouad, M. Jawaid, et al., Evaluation of characterisation efficiency of natural fibre-reinforced polylactic acid biocomposites for 3D printing applications, Sustain. Mater. Technol. 36 (2023) e00620.
[3] S. Ravanbod, K. Rahmani, S. Karmel, I. Pande, H. Amel, C. Branfoot, et al., From coral to control: bio-inspired, 3D-printable metamaterials with tuneable quasi-zero stiffness and multi-functional bio-composites, Mater. Des. 257 (2025) 114398.
[4] O. Akampumuza, P.M. Wambua, A. Ahmed, W. Li, X.H. Qin, Review of the applications of biocomposites in the automotive industry, Polym. Compos. 38 (11) (2017) 2553–2569.
[5] S. Sivakumar, V. Vignesh, I.V. Arasu, G. Venkatesan, B.R. Mohamed Rabi, Khan M. Adam, Experimental investigation on tensile and flexural properties of randomly oriented treated Palmyra fibre reinforced polyester composites, Mater. Today Proc. 46 (2021) 7556–7560.
[6] E.A.R. Zuiderveen, K.J.J. Kuipers, C. Caldeira, S.V. Hanssen, M.K. van der Hulst, M.M.J. de Jonge, et al., The potential of emerging bio-based products to reduce environmental impacts, Nat. Commun. 14 (1) (2023) 8521.
[7] W. Ahmad, S.J. McCormack, A. Byrne, Biocomposites for sustainable construction: A review of material properties, applications, research gaps, and contribution to circular economy, J. Build. Eng. 105 (2025) 112525.
[8] S. Başaran, İ. Türkmen, T. Yağcı, K. Kanbur, S.B. Baştürk, Comparative study on the thermal and tribological properties of PA12 and PA11 for coating applications, J. Appl. Polym. Sci. 141 (45) (2024) e56197.
[9] Y. Lebaupin, T.-Q.T. Hoang, M. Chauvin, F. Touchard, Influence of the stacking sequence on the low-energy impact resistance of flax/PA11 composite, J. Compos. Mater. 53 (22) (2019) 3187–3198.
[10] P. Venkatraman, A.M. Gohn, A.M. Rhoades, E.J. Foster, Developing high performance PA 11/cellulose nanocomposites for industrial-scale melt processing, Compos. Part B Eng. 174 (2019) 106988.
[11] M.A. Kacem, M. Guebailia, N. Sabba, S. Abdi, M. Bodaghi, Assessing extraction methods and mechanical and physicochemical properties of Algerian Yucca fibers for sustainable composite reinforcement, Macromol. Mater. Eng. 309 (10) (2024) 2400082.
[12] G. Rajeshkumar, V. Vignesh, A.M.A. Mohan, S.V.N. Prasaadh, A. Poovarasan, M. I. Ammarullah, Performance analysis of NaOH-treated randomly oriented bauhinia Purpurea L Fiber/epoxy (BPFE) composites: mechanical and free vibration studies for biomedical applications, J. Nat. Fibers 22 (1) (2025) 2543119.
[13] T. VarunKumar, V. Vignesh, Rajesh kumar G, Nagaprasad N., Sustainable hybrid bio-powder reinforced vinyl ester composites: enhancing mechanical and vibrational properties using clamshell and eggshell filler for various engineering applications, Polym. Bull. 83 (2) (2025) 48.
[14] M.K. Moghaddam, E. Karimi, Structural and physical characteristics of the yucca fiber, J. Ind. Text. 51 (5_suppl) (2022), 8018S-34S.
[15] M. Akonda, S. Alimuzzaman, D.U. Shah, A.N.M.M. Rahman, Physico-mechanical, thermal and biodegradation performance of random flax/Polylactic acid and unidirectional flax/Polylactic acid biocomposites, Fibers 6 (4) (2018) 98.
[16] A. Yılmaz, H. Ozkan, F.E. Genceli Güner, Utilizing the potential of waste hemp reinforcement: investigating mechanical and thermal properties of polypropylene and polylactic acid biocomposites, ACS Omega 9 (8) (2024) 8818–8828.
[17] S. Somashekhar, G.C. Shanthakumar, M. Nagamadhu, Influence of Fiber content and screw speed on the mechanical characterization of jute fiber reinforced polypropylene composite using Taguchi method, Mater. Today Proc. 24 (2020) 2366–2374.
[18] M.A. Kacem, M. Guebailia, M.L. Dezaki, S. Abdi, N. Sabba, A. Zolfagharian, et al., Development and 3D printing of PLA bio-composites reinforced with short yucca fibers and enhanced thermal and dynamic mechanical performance, J. Mater. Res. Technol. 36 (2025) 1243–1258.
[19] V. Vignesh, N.B. Karthik Babu, A.M. Arun Mohan, S. Sathees Kumar, N. Nagaprasad, N. Ayrilmis, et al., Development of hybrid fiber-reinforced vinyl

ester composites for civil and automotive applications, Sci. Rep. 15 (1) (2025) 37174.
[20] G. Koronis, A. Silva, M. Fontul, Green composites: A review of adequate materials for automotive applications, Compos. Part B Eng. 44 (1) (2013) 120–127.
[21] M.J. John, S. Thomas, Biofibres and biocomposites, Carbohydr. Polym. 71 (3) (2008) 343–364.
[22] M.P.M. Dicker, P.F. Duckworth, A.B. Baker, G. Francois, M.K. Hazzard, P. M. Weaver, Green composites: A review of material attributes and complementary applications, Compos. A: Appl. Sci. Manuf. 56 (2014) 280–289.
[23] E. Varga, F. Palásti, A. Bata, D.I. Kis, F. Tajti, Polyamide 11 composites with surface-activated intact Mica structures for advanced applications, Polymers 17 (21) (2025) 2861.
[24] P.E. Imoisili, T.-C. Jen, Mechanical and water absorption behaviour of potassium permanganate (KMnO4) treated plantain (Musa paradisiacal) fibre/epoxy bio-composites, J. Mater. Res. Technol. 9 (4) (2020) 8705–8713.
[25] A. Seile, E. Spurina, M. Sinka, Reducing global warming potential impact of bio-based composites based of LCA, Fibers 10 (9) (2022) 79.
[26] N.S. Kahigi, J.J. Mkunda, M.F. Mwema, R. Machunda, A comprehensive life cycle assessment of sisal yarn production: unveiling sustainability and resource optimization hotspots, Environ. Chall. 18 (2025) 101085.
[27] A.R. Rozyanty, S.F. Zhafer, Z. Shayfull, I. Nainggolan, L. Musa, L.T. Zheing, Effect of water and mechanical retting process on mechanical and physical properties of kenaf bast fiber reinforced unsaturated polyester composites, Compos. Struct. 257 (2021) 113384.
[28] Z. Leman, S.M. Sapuan, M.R. Ishak, M.M.H.M. Ahmad, Pre-treatment by water retting to improve the interfacial bonding strength of sugar palm fibre reinforced epoxy composite, Polymers Renew. Resour. 1 (1) (2010) 35–45.
[29] O. Olanrewaju, I.O. Oladele, S.O. Adelani, A comprehensive review on plant and animal fiber reinforced composites: experimental and theoretical approaches to interfacial strength optimization and potential applications, Hybrid Adv. 10 (2025) 100474.
[30] J. DG, V. V, M. Hashem, H. Fouad, Statistical approach to explore sustainable characteristics of cellulosic Desmostachya bipinnata fiber and its chemically modified conditions, Mater. Res. Express 11 (9) (2024) 095302.
[31] Y. Yao, S. Chen, The effects of fiber's surface roughness on the mechanical properties of fiber-reinforced polymer composites, J. Compos. Mater. 47 (23) (2013) 2909–2923.
[32] M. Balkundhi, S.S. Baloor, G. Bolar, Assessment of surface treatment methods for strengthening the interfacial adhesion in CARALL fiber metal laminates, Sci. Rep. 14 (1) (2024) 30909.
[33] L. Schraa, C. Rodricks, G. Kalinka, K. Roetsch, C. Scheffler, A. Sambale, et al., Characterisation and modelling of the fibre-matrix interface of short fibre reinforced thermoplastics using the push-out technique, Compos. Part B Eng. 297 (2025) 112317.
[34] I. Goda, E. Padayodi, R.N. Raoelison, Enhancing fiber/matrix interface adhesion in polymer composites: mechanical characterization methods and progress in interface modification, J. Compos. Mater. 58 (29) (2024) 3077–3110.
[35] H. Fallahi, O. Kaynan, A. Asadi, Insights into the effect of fiber–matrix interphase physiochemical- mechanical properties on delamination resistance and fracture toughness of hybrid composites, Compos. A: Appl. Sci. Manuf. 166 (2023) 107390.
[36] B. Ucpinar Durmaz, A. Aytac, Investigation of the mechanical, thermal, morphological and rheological properties of bio-based polyamide11/poly(lactic acid) blend reinforced with short carbon fiber, Mater. Today Commun. 30 (2022) 103030.
[37] Godara S.S. Mukesh, Effect of chemical modification of fiber surface on natural fiber composites: A review, Mater. Today Proc. 18 (2019) 3428–3434.
[38] T. Aziz, A. Ullah, H. Fan, M.I. Jamil, F.U. Khan, R. Ullah, et al., Recent Progress in Silane coupling agent with its emerging applications, J. Polym. Environ. 29 (11) (2021) 3427–3443.
[39] M. Bahrami, J. Abenojar, M.A. Martínez, Comparative characterization of hot-pressed polyamide 11 and 12: mechanical, thermal and durability properties, Polymers 13 (20) (2021) 3553.
[40] R. Androsch, C. Schick, Hydrogen-bond density controlled sub-Tg annealing peaks in fast-scanning-chip calorimeter heating scans of non-crystallized aliphatic polyamides, Thermochim. Acta 748 (2025) 179997.
[41] Mpd Lazari, AhMdFTd Silva, RhdS Garcia, ScdS Teixeira, Jed Oliveira, É. G. Chaves, et al., New insight into the microstructure changes and molecular mobility of polyamides exposed to H2S scavengers, Polymers 17 (12) (2025) 1634.
[42] R. Ma, L. Zhang, Z. Zhang, C. Huang, H. Huang, W. Cao, et al., Thermal-induced structural evolution of melt-stretched PA11: direct evidence for the preservation of hydrogen-bonded sheets above the brill transition temperature, Macromolecules 58 (1) (2025) 459–472.
[43] B. Wang, T. Wen, X. Zhang, A. Tercjak, X. Dong, A.J. Müller, et al., Nucleation of poly(lactide) on the surface of different fibers, Macromolecules 52 (16) (2019) 6274–6284.
[44] X. Yang, S.K. Biswas, J. Han, S. Tanpichai, M.C. Li, C. Chen, et al., Surface and interface engineering for nanocellulosic advanced materials, Adv. Mater. 33 (28) (2021) 2002264.
[45] S.F. Ferdous, M.F. Sarker, A. Adnan, Role of nanoparticle dispersion and filler-matrix interface on the matrix dominated failure of rigid C60-PE nanocomposites: A molecular dynamics simulation study, Polymer 54 (10) (2013) 2565–2576.
[46] A. Jabbarzadeh, The origins of enhanced and retarded crystallization in nanocomposite polymers, Nanomaterials 9 (10) (2019) 1472.
[47] A. Stalin, S. Mothilal, V. Vignesh, K.J. Nagarajan, T. Karthick, Mechanical properties of Typha Angustata/ vetiver/Banana Fiber mat reinforced vinyl Ester hybrid composites, J. Nat. Fibers 19 (13) (2022) 5227–5238.
[48] Z.-M. Huang, W.-J. Guo, H.-B. Huang, C.-C. Zhang, Tensile strength prediction of short Fiber reinforced composites, Materials 14 (11) (2021) 2708.
[49] C. Brauner, T. Bourquin, J. Kupski, L. Zweifel, M. Hajikazemi, C. Houwink, et al., Additive Manufacturing of Bio-Based PA11 Composites with Recycled Short Carbon Fibers: Stiffness–Strength Characterization, Polymers 17 (18) (2025) 2549.
[50] F. Asoodeh, M. Aghvami-Panah, S. Salimian, M. Naeimirad, khoshnevis H, Zadhoush A., The Effect of Fibers' Length Distribution and Concentration on Rheological and Mechanical Properties of Glass Fiber–Reinforced Polypropylene Composite, J. Ind. Text. 51 (5_suppl) (2022), 8452S-71S.
[51] S. Lu, B. Zhang, J. Niu, C. Yang, C. Sun, L. Wang, et al., Effect of fiber content on mechanical properties of carbon fiber-reinforced polyether-ether-ketone composites prepared using screw extrusion-based online mixing 3D printing, Addit. Manuf. 80 (2024) 103976.
[52] X. Chen, X. Wang, X. Luo, L. Chen, Y. Li, J. Xu, et al., Bamboo as a naturally-optimized fiber-reinforced composite: interfacial mechanical properties and failure mechanisms, Compos. Part B Eng. 279 (2024) 111458.
[53] M. Martínez-Sanz, F. Pettolino, B. Flanagan, M.J. Gidley, E.P. Gilbert, Structure of cellulose microfibrils in mature cotton fibres, Carbohydr. Polym. 175 (2017) 450–463.
[54] T. Huber, N. Graupner, J. Müssig, Regenerated cellulose fibres and their composites: from fundamental properties to advanced applications, Prog. Mater. Sci. 156 (2026) 101547.
[55] A. Jäger, T. Bader, K. Hofstetter, J. Eberhardsteiner, The relation between indentation modulus, microfibril angle, and elastic properties of wood cell walls, Compos. A: Appl. Sci. Manuf. 42 (6) (2011) 677–685.
[56] S. Yaisun, T. Trongsatitkul, PLA-based hybrid biocomposites: effects of fiber type, fiber content, and annealing on thermal and mechanical properties, Polymers 15 (20) (2023) 4106.
[57] M.Z. Rahman, M. Rahman, T. Mahbub, M. Ashiquzzaman, S. Sagadevan, M. E. Hoque, Advanced biopolymers for automobile and aviation engineering applications, J. Polym. Res. 30 (3) (2023) 106.
[58] S. Rohner, J. Humphry, C.M. Chaléat, L.-J. Vandi, D.J. Martin, N. Amiralian, et al., Mechanical properties of polyamide 11 reinforced with cellulose nanofibres from Triodia pungens, Cellulose 25 (4) (2018) 2367–2380.
[59] D.M. Panaitescu, R.A. Gabor, A.N. Frone, E. Vasile, Influence of thermal treatment on mechanical and morphological characteristics of polyamide 11/ cellulose nanofiber nanocomposites, J. Nanomater. 2015 (1) (2015) 136204.
[60] D. Van Cong, N.V. Giang, T.H. Trung, T. Hoang, T.D. Lam, D.Q. Tham, et al., Biocomposites from polyamide 11 reinforced by organic silane modified jute fibers: fabrication and characterization, J. Appl. Polym. Sci. 139 (11) (2022) 51795.
[61] D. Manikandan, V.C. Sathish Gandhi, R. Kumaravelan, V. Vignesh, Effect of hybrid filler loading (Polyalthia longifolia seed and graphite) on the mechanical and thermal properties of vinyl ester composites, Polym. Compos. 45 (7) (2024) 6318–6331.
[62] R. Benamrane, M.S. Bennouna, S. Alleg, M. Fellah, A. Boumaza, S. Guessasma, Experimental study of a new cellulose fiber extracted from Iris pallida Lam, Cellulose (2025), https://doi.org/10.1007/s10570-025-06885-1 in Press.
[63] K. Nasri, É. Loranger, L. Toubal, Effect of cellulose and lignin content on the mechanical properties and drop-weight impact damage of injection-molded polypropylene-flax and -pine fiber composites, J. Compos. Mater. 57 (21) (2023) 3347–3364.
[64] J. Ou, C. Feng, Y. Shao, Z. Ni, Q. Wang, X. Yan, The regulating effect of cellulose nanofibers on the structure and properties of polylactic acid/bio-nylon 11 composites, Polym. Compos. (2025).
[65] N.A.M. Razali, R. Mohd Sohaimi, R.N.I.R. Othman, N. Abdullah, S.Z.N. Demon, L. Jasmani, et al., Comparative study on extraction of cellulose Fiber from Rice straw waste from chemo-mechanical and pulping method, Polymers 14 (3) (2022) 387.
[66] M. Akhlaq, M. Uroos, Evaluating the impact of cellulose extraction via traditional and Ionosolv pretreatments from domestic matchstick waste on the properties of Carboxymethyl cellulose, ACS Omega 8 (9) (2023) 8722–8731.
[67] K. Rahmani, C. Branfoot, M. Bodaghi, Bio-derived PA11/bamboo charcoal/glass fibre composites for fused filament fabrication, warpage control, strength and flame retardancy, Virtual Phys. Prototyp. 20 (1) (2025) e2589848.
[68] V. Gigante, F. Cartoni, B. Dal Pont, L. Aliotta, Extrusion parameters optimization and mechanical properties of bio-polyamide 11-based biocomposites reinforced with short basalt fibers, Polymers 16 (21) (2024) 3092.
[69] M. Dobrosielska, R. Dobrucka, D. Brząkalski, P. Kozera, A. Martyła, E. Gabriel, et al., Polyamide 11 composites reinforced with diatomite biofiller—mechanical, rheological and crystallization properties, Polymers 15 (6) (2023) 1563.
[70] A.Y. Al-Maharma, P. Sendur, Review of the main factors controlling the fracture toughness and impact strength properties of natural composites, Mater. Res. Express 6 (2) (2018) 022001.
[71] V. Vignesh, A.N. Balaji, B.R. Mohamed Rabi, N. Rajini, N. Ayrilmis, M.K. V. Karthikeyan, et al., Cellulosic fiber based hybrid composites: A comparative investigation into their structurally influencing mechanical properties, Constr. Build. Mater. 271 (2021) 121587.
[72] S. AhmadvashAghbash, I. Verpoest, Y. Swolfs, M. Mehdikhani, Methods and models for fibre–matrix interface characterisation in fibre-reinforced polymers: a review, Int. Mater. Rev. 68 (8) (2023) 1245–1319.

[73] G. Zhang, P. Suwatnodom, J. Ju, Micromechanics of crack bridging stress-displacement and fracture energy in steel hooked-end fiber-reinforced cementitious composites, Int. J. Damage Mech. 22 (6) (2013) 829–859.
[74] T. Islam, M.H. Chaion, M.A. Jalil, A.S. Rafi, F. Mushtari, A.K. Dhar, et al., Advancements and challenges in natural fiber-reinforced hybrid composites: a comprehensive review, SPE Polymers 5 (4) (2024) 481–506.
[75] S. Hajibabazadeh, H. Ghaleh, M.M. Mazidi, M.K. Razavi Aghjeh, Phase structure, mechanical properties and failure behavior of compatibilized polylactide/polyamide 11 systems, Polym. Eng. Sci. 65 (3) (2025) 1214–1227.
[76] A.H. Abdel Kader, T.Y.A. Fahmy, S. Kamel, Lignocellulosic reinforced composites: a snapshot of progress, J. Wood Chem. Technol. 45 (4) (2025) 167–195.
[77] S. Sadashiv Todkar, Patil S. Abasaheb, Creep and heat deflection temperature (HDT) study of pineapple leaf fibre (PALF) and montmorillonite (MMT) nanoclay reinforced poly-lactic acid (PLA) based laminated hybrid biocomposite, Mater. Today Proc. 62 (2022) 7534–7539.
[78] L. Aliotta, M. Gasenge, V. Gigante, A. Lazzeri, Micromechanical deformation processes and failure of PBS based composites containing ultra-short cellulosic fibers for injection molding applications, Polymers 14 (21) (2022) 4499.
[79] M.M. Kabir, M.Y. Alhaik, S.H. Aldajah, K.T. Lau, H. Wang, M.M. Islam, Effect of hemp fibre surface treatment on the fibre-matrix Interface and the influence of cellulose, hemicellulose, and lignin contents on composite strength properties, Adv. Mater. Sci. Eng. 2021 (1) (2021) 9753779.
[80] A.H. Alias, M.N. Norizan, F.A. Sabaruddin, M.R.M. Asyraf, M.N.F. Norrrahim, A. R. Ilyas, et al., Hybridization of MMT/lignocellulosic fiber reinforced polymer nanocomposites for structural applications: a review, Coatings 11 (11) (2021) 1355.
[81] Z. Osman, M. Elamin, E. Ghorbel, B. Charrier, Influence of alkaline treatment and Fiber morphology on the mechanical, physical, and thermal properties of polypropylene and Polylactic acid biocomposites reinforced with Kenaf, bagasse, hemp fibers and softwood, Polymers 17 (7) (2025) 844.
[82] A. Gallos, G. Paës, F. Allais, J. Beaugrand, Lignocellulosic fibers: a critical review of the extrusion process for enhancement of the properties of natural fiber composites, RSC Adv. 7 (55) (2017) 34638–34654.
[83] T. Amornsakchai, S. Duangsuwan, Upcycling of HDPE Milk bottles into high-stiffness, high-HDT composites with pineapple leaf waste materials, Polymers 15 (24) (2023) 4697.
[84] H. Baniasadi, S. Lipponen, M. Asplund, J. Seppälä, High-concentration lignin biocomposites with low-melting point biopolyamide, Chem. Eng. J. 451 (2023) 138564.
[85] M.A. Bashir, Use of dynamic mechanical analysis (DMA) for characterizing interfacial interactions in filled polymers, Solids 2 (1) (2021) 108–120.
[86] M. Jawaid, S. Awad, A.S. Ismail, M. Hashem, H. Fouad, I. Uddin, Effect of kenaf fibre loading on thermal and dynamic mechanical properties of bio epoxy composites, J. Therm. Anal. Calorim. 149 (19) (2024) 10441–10448.
[87] G. Barrera, L.L. Paim, R.J. dos Santos, F.C. Cabrera, E.P. dos Reis, J.C. Sánchez, et al., The effect of surface treatments on the mechanical properties of low-density polyethylene/natural rubber composites reinforced with sugarcane bagasse ash, J. Compos. Sci. 9 (9) (2025) 489.
[88] M.A. Sattar, Interface structure and dynamics in polymer-nanoparticle hybrids: A review on molecular mechanisms underlying the improved interfaces, ChemistrySelect 6 (20) (2021) 5068–5096.
[89] M.C. Righetti, M. Vannini, A. Celli, D. Cangialosi, C. Marega, Bio-based semi-crystalline PEF: temperature dependence of the constrained amorphous interphase and amorphous chain mobility in relation to crystallization, Polymer 247 (2022) 124771.
[90] P. Krishnasamy, G R, Belaadi A, R S., Dynamic mechanical characteristics of natural fiber hybrid composites, bio composites and nano composites –a review, Eng. Res. Express 6 (1) (2024) 012503.
[91] J.-S. Kim, A.H. Muliana, A combined viscoelastic–viscoplastic behavior of particle reinforced composites, Int. J. Solids Struct. 47 (5) (2010) 580–594.
[92] H. Oliver-Ortega, J.A. Méndez, P. Mutjé, Q. Tarrés, F.X. Espinach, M. Ardanuy, Evaluation of thermal and thermomechanical behaviour of bio-based polyamide 11 based composites reinforced with lignocellulosic Fibres, Polymers 9 (10) (2017) 522.
[93] S. Koutsoumpis, K.N. Raftopoulos, O. Oguz, C.M. Papadakis, Y.Z. Menceloglu, P. Pissis, Dynamic glass transition of the rigid amorphous fraction in polyurethane-urea/SiO 2 nanocomposites, Soft Matter 13 (26) (2017) 4580–4590.
[94] A.M. Salaberría, R. Teruel-Juanes, J.D. Badia, S.C.M. Fernandes, V. Sáenz de Juano-Arbona, J. Labidi, et al., Influence of chitin nanocrystals on the dielectric behaviour and conductivity of chitosan-based bionanocomposites, Compos. Sci. Technol. 167 (2018) 323–330.
[95] A.E. Krauklis, C.W. Karl, I.B.C.M. Rocha, J. Burlakovs, R. Ozola-Davidane, A. I. Gagani, et al., Modelling of environmental ageing of polymers and polymer composites—modular and multiscale methods, Polymers 14 (1) (2022) 216.
[96] P.H. Nguyen, S. Spoljaric, J. Seppälä, Redefining polyamide property profiles via renewable long-chain aliphatic segments: towards impact resistance and low water absorption, Eur. Polym. J. 109 (2018) 16–25.
[97] M. Jacob, S. Joseph, L.A. Pothan, S. Thomas, A study of advances in characterization of interfaces and fiber surfaces in lignocellulosic fiber-reinforced composites, Compos. Interfaces 12 (1–2) (2005) 95–124.
[98] R. Qin, D. Lau, Evaluation of the moisture effect on the material interface using multiscale modeling, Multiscale Sci. Eng. 1 (2) (2019) 108–118.
[99] M. Mohammed, AjaM Jawad, A.M. Mohammed, J.K. Oleiwi, T. Adam, A. F. Osman, et al., Challenges and advancement in water absorption of natural fiber-reinforced polymer composites, Polym. Test. 124 (2023) 108083.
[100] S. Islam, F.E. Karim, M.R. Islam, Assessing the consequences of water retention on the structural integrity of jute fiber and its composites: A review, SPE Polymers 5 (4) (2024) 457–480.
[101] D. Gunwant, Moisture resistance treatments of natural fiber-reinforced composites: a review, Compos. Interfaces 31 (8) (2024) 979–1047.
[102] M.L. Di Lorenzo, A. Longo, R. Androsch, Polyamide 11/poly(butylene succinate) bio-based polymer blends, Materials 12 (17) (2019) 2833.
[103] X.Y. Du, Q. Li, G. Wu, S. Chen, Multifunctional micro/nanoscale fibers based on microfluidic spinning technology, Adv. Mater. 31 (52) (2019) 1903733.
[104] C.H. Lee, A. Khalina, S.H. Lee, Importance of interfacial adhesion condition on characterization of plant-Fiber-reinforced polymer composites: A review, Polymers 13 (3) (2021) 438.
[105] S. Tawfick, M. De Volder, D. Copic, S.J. Park, C.R. Oliver, E.S. Polsen, et al., Engineering of micro-and nanostructured surfaces with anisotropic geometries and properties, Adv. Mater. 24 (13) (2012) 1628–1674.
[106] M.A. Musthaq, H.N. Dhakal, Z. Zhang, A. Barouni, R. Zahari, The effect of various environmental conditions on the impact damage behaviour of natural-fibre-reinforced composites (NFRCs)—A critical review, Polymers 15 (5) (2023) 1229.
[107] L. Sang, Y. Wang, C. Wang, X. Peng, W. Hou, L. Tong, Moisture diffusion and damage characteristics of carbon fabric reinforced polyamide 6 laminates under hydrothermal aging, Compos. A: Appl. Sci. Manuf. 123 (2019) 242–252.
[108] L. Monson, M. Braunwarth, C. Extrand, Moisture absorption by various polyamides and their associated dimensional changes, J. Appl. Polym. Sci. 107 (1) (2008) 355–363.
[109] N. Obaid, M.T. Kortschot, M. Sain, Understanding the stress relaxation behavior of polymers reinforced with short elastic fibers, Materials 10 (5) (2017) 472.
[110] V. Popineau, A. Célino, M. Péron, C. Baley, A. Le Duigou, Understanding the effect of hygroscopic cycling on the internal stress and stiffness of natural fibre biocomposites, Compos. A: Appl. Sci. Manuf. 158 (2022) 106995.
[111] A.H. Karoyo, L.D. Wilson, A review on the design and hydration properties of natural polymer-based hydrogels, Materials 14 (5) (2021) 1095.
[112] A.A. Bachchan, P.P. Das, V. Chaudhary, Effect of moisture absorption on the properties of natural fiber reinforced polymer composites: A review, Mater. Today Proc. 49 (2022) 3403–3408.
[113] B. Praveena, S.V. Kumar, H. Manjunath, B. Sachin, S.P.S. Yadav, B.R. Lochan, et al., Investigation of moisture absorption and mechanical properties of natural fibre reinforced polymer hybrid composite, Mater. Today Proc. 45 (2021) 8219–8223.
[114] Y. Wu, J. Fajoui, P. Casari, S. Fréour, Characterization of the cyclic hygroscopic aging behavior of balsa wood core bio-composite sandwich structures with preexisting defects in laminate skins, Polym. Compos. 46 (2025) 13893–13906.
[115] L. Äkräs, F. Silvenius, H. Baniasadi, M. Vahvaselkä, H. Ilvesniemi, J. Seppälä, A cradle-to-gate life cycle assessment of polyamide-starch biocomposites: carbon footprint as an indicator of sustainability, Clean Techn. Environ. Policy 26 (10) (2024) 3297–3312.
[116] B.K. Sovacool, M.D. Bazilian, J. Kim, S. Griffiths, Six bold steps towards net-zero industry, Energy Res. Soc. Sci. 99 (2023) 103067.
[117] M. Pervaiz, M.M. Sain, Carbon storage potential in natural fiber composites, Resour. Conserv. Recycl. 39 (4) (2003) 325–340.
[118] M. Latos-Brozio, K. Rułka, A. Masek, Review of bio-fillers dedicated to polymer compositions, Chem. Biodivers. 22 (2025) e202500406.
[119] S. Motamedi, D.R. Rousse, G. Promis, A review of mycelium bio-composites as energy-efficient sustainable building materials, Energies 18 (16) (2025) 4225.
[120] R. Chauhan, R. Sartape, N. Minocha, I. Goyal, M.R. Singh, Advancements in environmentally sustainable technologies for ethylene production, Energy Fuel 37 (17) (2023) 12589–12622.
[121] E. Bontempi, A new approach for evaluating the sustainability of raw materials substitution based on embodied energy and the CO2 footprint, J. Clean. Prod. 162 (2017) 162–169.
[122] J. Xu, X. Gao, C. Zhang, S. Yin, Flax fiber-reinforced composite lattice cores: A low-cost and recyclable approach, Mater. Des. 133 (2017) 444–454.
[123] M. Kadam, A. Kulkarni, K. Vaidya, B. Kandasubramanian, Eco-functional hybrid composites: synergistic reinforcement of recycled polypropylene via glass Fiber and agro-waste activated carbon under circular economy principles, Next Res. 2 (2025) 100835.
[124] K. Amulya, R. Katakojwala, S. Ramakrishna, S.V. Mohan, Low carbon biodegradable polymer matrices for sustainable future, Compos. Part C Open Access 4 (2021) 100111.
[125] M. Çevik, A.N. Diambu, Advancing sustainable development goals through the use of biocomposites for a greener future, Sci. Res. Rep. (2024) 1.
[126] M.A. Alam, S. Sapuan, H. Ya, P. Hussain, M. Azeem, R. Ilyas, Application of biocomposites in automotive components: A review, Biocompos. Synth. Compos. Automot. Applic. (2021) 1–17.
[127] P. Roy, F. Defersha, A. Rodriguez-Uribe, M. Misra, A.K. Mohanty, Evaluation of the life cycle of an automotive component produced from biocomposite, J. Clean. Prod. 273 (2020) 123051.
[128] M. Faheem, K.A. Khan, Harnessing sustainable biocomposites: a review of advances in greener materials and manufacturing strategies, Polym. Bull. 1-44 (2025).
[129] J. Pryshlakivsky, C. Searcy, Fifteen years of ISO 14040: a review, J. Clean. Prod. 57 (2013) 115–123.
[130] Y.V. Thorat, S.S. Chavan, D.D. Mohite, U.S. Pawar, Development of eco-friendly bio-composites using banana fibers for enhanced tensile and flexural properties, Mater. Today Proc. (2024), https://doi.org/10.1016/j.matpr.2024.04.061 in Press.